

Evaluation of ultrafine particle concentrations and size distributions at London Heathrow Airport

Stacey, Brian; Harrison, Roy M.; Pope, Francis

DOI:

[10.1016/j.atmosenv.2019.117148](https://doi.org/10.1016/j.atmosenv.2019.117148)

License:

Creative Commons: Attribution-NonCommercial-NoDerivs (CC BY-NC-ND)

Document Version

Peer reviewed version

Citation for published version (Harvard):

Stacey, B, Harrison, RM & Pope, F 2020, 'Evaluation of ultrafine particle concentrations and size distributions at London Heathrow Airport', *Atmospheric Environment*, vol. 222, 117148.

<https://doi.org/10.1016/j.atmosenv.2019.117148>

[Link to publication on Research at Birmingham portal](#)

General rights

Unless a licence is specified above, all rights (including copyright and moral rights) in this document are retained by the authors and/or the copyright holders. The express permission of the copyright holder must be obtained for any use of this material other than for purposes permitted by law.

- Users may freely distribute the URL that is used to identify this publication.
- Users may download and/or print one copy of the publication from the University of Birmingham research portal for the purpose of private study or non-commercial research.
- User may use extracts from the document in line with the concept of 'fair dealing' under the Copyright, Designs and Patents Act 1988 (?)
- Users may not further distribute the material nor use it for the purposes of commercial gain.

Where a licence is displayed above, please note the terms and conditions of the licence govern your use of this document.

When citing, please reference the published version.

Take down policy

While the University of Birmingham exercises care and attention in making items available there are rare occasions when an item has been uploaded in error or has been deemed to be commercially or otherwise sensitive.

If you believe that this is the case for this document, please contact UBIRA@lists.bham.ac.uk providing details and we will remove access to the work immediately and investigate.

1
2
3
4
5
6 **Evaluation of Ultrafine Particle Concentrations**
7 **and Size Distributions at London Heathrow**
8 **Airport**

9
10 **Brian Stacey^{*,1}, Roy M. Harrison² and Francis Pope**

11
12 **Division of Environmental Health and Risk Management,**
13 **School of Geography, Earth and Environmental Sciences**
14 **University of Birmingham**
15 **Edgbaston, Birmingham B15 2TT**
16 **United Kingdom**
17
18
19

* To whom correspondence should be addressed.
Email: Brian.Stacey@ricardo.com

¹Also at Ricardo Energy and Environment, The Gemini Building, Fermi Avenue, Harwell, Didcot, Oxfordshire, OX11 0QR, United Kingdom

²Also at: Department of Environmental Sciences / Center of Excellence in Environmental Studies, King Abdulaziz University, PO Box 80203, Jeddah, 21589, Saudi Arabia

20 **ABSTRACT**

21 A study to monitor UFP at Heathrow Airport was undertaken in the autumn of 2016. The objective
22 was to assess the context of measurements at the airport compared to measurements at “typical”
23 traffic, background and rural locations in the south east of England. Measurements were made at
24 two airport locations (called LHR2 and Oaks Road) at opposite ends of the airfield, to further
25 understand the contribution of the airport to local air quality. Average concentrations showed that
26 total particle number concentrations at the airport are typically lower than a traffic location and
27 higher than an urban background location in London, matching the trends seen for NO_x, PM₁₀,
28 PM_{2.5} and BC pollutants. However, the size distribution of the submicrometre particles at the airport
29 is completely different to the London monitoring stations, with the airport PSD dominated by
30 particles with a mode of 20nm. In contrast, measurements of PN in London have a significantly
31 larger mode of 30nm. This study demonstrated that measurements of particle number from within
32 the airport perimeter are dominated by the smallest particles and are closely associated with aircraft.
33 Analysis of the operating modes at the airport showed that aircraft departing from the airport emit
34 particles in much higher numbers than those arriving. Nucleation mode particles are commonly
35 associated with emissions from combustion processes. However, measurement of these particles at
36 the airport are not strongly correlated with Black Carbon. There does appear to be some
37 correlation of nucleation mode particles with UV active BC particles (brown carbon, typically
38 associated with biomass combustion or wood smoke) at the Heathrow airside monitoring station,
39 LHR2. There is also modest association between nucleation mode particles and NO₂. The study
40 showed that the classical air pollutants measured at Heathrow are very similar in concentration to
41 typical urban environments in London and south east England, but particle numbers in the sub
42 30nm size range are markedly different to those measured in London.

43
44
45

46 **1. INTRODUCTION**

47 Heathrow Airport is the busiest two-runway airport in the world. In 2016, the airport handled over
48 75.7 million passengers and approximately 470,000 aircraft movements

49 ([https://www.heathrow.com/file_source/Company/Static/PDF/Investorcentre/Heathrow-\(SP\)-
50 FY2016-results-release-\(FINAL\).pdf](https://www.heathrow.com/file_source/Company/Static/PDF/Investorcentre/Heathrow-(SP)-FY2016-results-release-(FINAL).pdf)).

51

52 Heathrow Airport has undertaken automatic monitoring of air quality continuously since 1992. In
53 2016, there were 4 locations around the airport. These focus on classical air pollutants; NO, NO₂,
54 PM₁₀ and PM_{2.5}. Black Carbon is measured at 2 of the 4 locations, while O₃ and meteorological
55 measurements are each measured at one station. This data and background information is available
56 to view and download at <http://heathrowairwatch.org.uk>.

57

58 The literature review by Stacey (2019) collects the most relevant literature into a single document
59 and informs the direction of research and analysis throughout this paper. Evidence, for example
60 from Fanning et al. (2007), Fleuti et al. (2017), Hudda and Fruin (2016), Masiol et al. (2017) and
61 Peters et al. (2016), identifies that concentrations of ultrafine particles (UFP) close to airports are
62 substantially different to UFP concentrations in more conventional urban environments.

63

64 As of the end of 2015, the literature was incomplete in the identification, assessment and nature of
65 the ambient concentrations of UFP emitted from airports and aircraft. Research conducted by, for
66 example, Donaldson et al. (2001) and Health Effects Institute (2013) has identified links between
67 exposure to UFP and detrimental health impact and specifically argue that the smallest particles are
68 likely to carry the highest risk to adverse health outcome. These health impact studies focussed
69 primarily on particles emitted from road transport and energy use into the ambient environment –
70 few studies had been conducted on the health impact of exposure to UFP around airports.

71 Ellermann et al. (2011) undertook research at Copenhagen Airport to assess exposure of airport
72 workers, but no associations with health impacts were presented in that report.

73

74 Studies undertaken by, for example Durdina et al. (2014), Lobo et al. (2015), Abegglen et al.
75 (2016), Turgut et al. (2015), and Vander Wal et al. (2016), measured emissions directly from the
76 exhaust of aircraft. These largely focussed on non-volatile particles and showed that, generally,
77 these particles are mostly carbon based and not significantly different in composition to other
78 combustion sources.

79

80 As the exhaust plume emerges from the engine and interacts with the atmosphere, combustion
81 products cool and can condense and/or interact with other components to form secondary aerosols.
82 A study by Beyersdorf et al. (2014), looked at volatile and non-volatile UFP exhaust emissions with
83 increasing distance from the source and found that as the exhaust plume cools and evolves, large
84 quantities of very fine particles are detected.

85

86 Studies of ambient concentrations by, for example Ellermann et al. (2012), Fanning et al. (2007),
87 Hudda and Fruin (2016), Westerdahl et al. (2008), Peters et al. (2016), Keuken et al. (2015),
88 Bezemer et al. (2015), Riley et al. (2016), Fleuti et al. (2017), and Shirmohammadi et al. (2017),
89 have all shown that high PN concentrations can be seen close to airports.

90

91 Masiol et al. (2017) undertook a pair of studies at Harlington, 1 km north of the airport in 2014 and
92 2015, which further confirmed that emissions of UFP from airports are different in size distribution
93 to typical urban and road traffic environments. The studies led by Hudda, Peters, Keuken and
94 Bezemer all showed that the finest particles emitted from aircraft remain in the atmosphere and can
95 be transported over large distances downwind of an airport. Hudda and Fruin (2016) were able to
96 detect airport related UFP emissions 18 km from Los Angeles International Airport, LAX , while

97 the Keuken et al. (2015) research detected airport related UFP over 40 km from Amsterdam Airport
98 Schiphol .

99

100 Assessment of the research by Masiol and others made it clear that further robust investigation of
101 UFP measurements, and in particular the particle size distribution of aircraft emissions was
102 warranted. This paper presents the results from the measurement campaign, undertaken between
103 September and November 2016, to determine UFP concentrations and size distributions near the
104 airport.

105

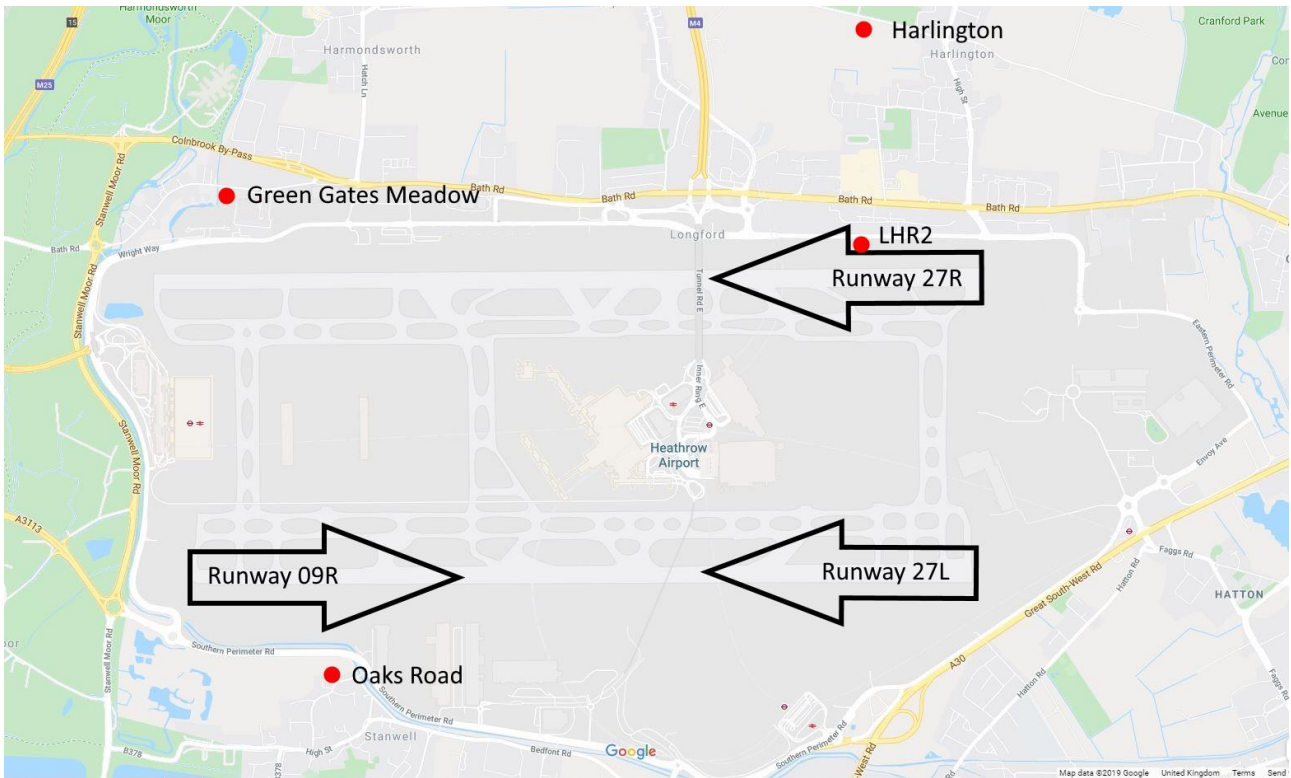
106 **2. METHODS**

107 **2.1 Monitoring Locations**

108 This measurement campaign was designed to compare measurements of UFP at Heathrow against
109 measurements made at other measurement stations in the South East of the UK, and then to further
110 explore the local nature of UFP at the airport.

111 The network of air quality monitoring stations at Heathrow Airport is presented in Figure 1:

112



113

114 **Figure 1.** Locations of Heathrow monitoring stations. Runway 27R, Runway 27L and Runway
 115 09R denote the three operating modes of the airport, indicating here the runway assigned for
 116 departing aircraft. Note that aircraft never depart in an easterly direction on the northern runway.
 117

118 Because of the dominant south-westerly nature of the winds in the UK, two of the four locations are
 119 ideally suited to explore the contribution of the airport to local air quality; Oaks Road and LHR2.
 120

121 **Oaks Road** – Located in a residential area to the south west of the airport, approximately 600m
 122 from the southern runway. It has been in continuous operation since 2001, measuring PM₁₀, PM_{2.5},
 123 BC and NO_x.
 124

125 **LHR2** – located airside in the north eastern corner of the airfield, 170m from the northern runway
 126 and less than 20m from the northern perimeter road. It has operated continuously since 1993,
 127 measuring PM₁₀, PM_{2.5}, BC, NO_x and meteorology.
 128

129

130 **2.2 UFP Measurement Campaign**

131 Measurement of UFP at the LHR2 and Oaks Road monitoring stations was undertaken between 30th
132 September and 25th November 2016.

133

134 The following equipment was used:

- 135 • Butanol based TSI Model 3775 CPCs (TSI inc., MN, USA) to count particle numbers.
- 136 • At Oaks Road, TSI Model 3080 with long DMA (Model 3081) classifier and soft X-ray
137 neutraliser. Automatic on-board software correction was enabled for diffusive losses and
138 multiple charge. Analyser operation and data storage was managed on a laptop running AIM
139 v9.0.0.0, which was used to control the operation of the TSI Model 3080/ Model 3775 setup.
- 140 • At LHR2, TSI Model 3082 with long DMA (Model 3081) classifier and soft X-ray
141 neutraliser. Automatic on-board software correction was enabled for diffusive losses and
142 multiple charge. Analyser operation and data storage controlled by the Model 3082 running
143 AIM v10.1.0.6. Data was downloaded weekly from the 3082 to a USB stick for subsequent
144 analysis.

145 The operating methodology of the TSI Scanning Mobility Particle Sizer (SMPS) and
146 Condensation Particle Counter (CPC) has been extensively described in literature, for example
147 by Wiedensohler et al. (2012) and Wiedensohler et al. (2018). The only difference from the
148 recommendations of Wiedensohler et al. (2012) was the absence of a dryer.

149

150 Both SMPS instruments were configured to sample in the range 14.6nm to 661.2nm. Sampling was
151 programmed to run for 3 minutes, sweeping up in size for 2 minutes 15 seconds, and returning
152 down for the remaining 45 seconds.

153

154 Both instruments were set up to be operated continuously for the entire measurement campaign;
155 unattended automated operation 24 hours per day. Because of the proprietary nature of the TSI
156 software and only a short window of opportunity to deploy the analysers, it was not possible to

157 establish remote communication to the analysers. The monitoring stations were visited weekly to
158 ensure correct operation and take remedial action if required.

159

160 The Heathrow CPCs and SMPSs were calibrated before and after the monitoring campaign at the
161 ISO/IEC17025 accredited Ricardo Energy and Environment (REE) calibration laboratory in
162 Harwell, UK. The classifiers and CPC were calibrated using a Jing miniCAST model 6003 (Jing
163 Ltd, Zollikofen, Switzerland) soot generator, which creates particles using a controlled burn
164 propane flame. The results of these calibrations showed both CPCs were accurate to within 1% of
165 the reference device and the SMPSs were able to size particles within 1 size bin in the range 14.6nm
166 to 680nm.

167

168 **2.3 Differences between Heathrow and National Monitoring UFP analyser setup**

169 The configuration of the Heathrow analysers matched, as far as possible, the configurations used in
170 the UK Particle Number monitoring network (<https://uk-air.defra.gov.uk/interactive-map>). This
171 network is managed by Kings' College London, while operation and QA/QC is provided by the
172 National Physical Laboratory. The national network stations use the following equipment:

- 173 • Butanol based TSI 3775 Condensation Particle Counters (CPC)
- 174 • TSI 3080 Scanning Mobility Particle Sizer (SMPS) with long DMA classifier and Kr-85
175 neutraliser source
- 176 • Nafion dryer
- 177 • Laptop running AIM v9.0.0.0

178 The SMPS / CPCs in the national network are also configured to sample in the range 14.6nm to
179 661.2nm. Sampling is also programmed to run for 3 minutes, sweeping up in size for 2 minutes 15
180 seconds, and returning down for the remaining 45 seconds. This will allow measurements between
181 the airport and national network analysers to be directly and robustly compared with each other.

182 The authors believe that this is the first time such a robust concurrent comparison has been made
183 between UFP measured at airports and background locations.

184
185 In 2016, the 3 national network stations measuring UFP were located at:

- 186 • **London Marylebone Road** – a heavily trafficked roadside location, near Baker Street in the
187 centre of London.
- 188 • **London North Kensington** – located in a school in a residential area of West London, less
189 than 4km west of the Marylebone Road station.
- 190 • **Chilbolton Observatory** – located in a rural environment, 25km north of the centre of
191 Southampton, 78km WSW of Heathrow Airport and 95km from Marylebone Road.

192
193 There were two main differences between measurements made at Heathrow and those made in the
194 national network:

- 195 • A nafion dryer is used in the national network station analysers. As noted above, no drying
196 was installed in line for the Heathrow study. It was considered unnecessary: studies (e.g.
197 Stanier et al., 2004) have shown that relative humidity contributes little to increased particle
198 size even for hygroscopic particles smaller than 50nm.
- 199 • Because of transportation restrictions inside the airport, a radioactive source was impossible
200 to deploy. Comparison studies within CEN TC264 WG32 and ISO/TC24/SC4/WG12
201 (standards in development), show that the measurement differences between particles
202 neutralised with soft X-rays and those neutralised with beta radiation are negligible, adding
203 further confidence that the X-ray and beta radiation neutralisers behave in a reasonably
204 similar manner. Additionally, the calibration of the Heathrow analysers at REE was
205 undertaken using a Kr-85 neutraliser for the reference device. The close agreement of the
206 Heathrow analysers, for both counting and sizing, reinforces the confidence that field
207 measurements are valid.

208

209 **2.4 Data Analysis**

210 The plots and analysis undertaken in this paper make extensive use of the R and R Studio programs
211 (R Foundation for Statistical Computing, Vienna, Austria, and R Studio Inc, MA, USA) and the
212 OpenAir suite of analysis tools (Carslaw and Ropkins, (2012))

213

214 Unless specifically stated, particle number plots are aggregated into three size groups, defined here
215 as:

- 216 • Nucleation (particles smaller than 25nm),
- 217 • Aitken (particles between 26 and 100nm)
- 218 • Accumulation (particles larger than 100nm)

219

220 Measurements from the black carbon aethalometers are reported here from two of the seven
221 components:

- 222 • Black Carbon (BC) – the Particulate Matter concentration recorded from the attenuation of
223 light by particles in the infra-red spectrum at 880nm
- 224 • Ultra Violet Particulate Matter (UVPM) – defined here as the additional particulate matter
225 concentration recorded from the attenuation in the UV region of the spectrum. It is calculated
226 from the difference between the concentration recorded at 370nm and the concentration
227 recorded at 880nm using a wavelength-adjusted absorption coefficient. Some other studies
228 have referred to this variable as “Brown Carbon” or Delta-C and interpreted it as a measure of
229 wood smoke concentrations (e.g. Wang et al. (2011)):

230

$$231 \text{UVPM} = \text{Conc}_{\text{ATT } 370} - \text{Conc}_{\text{ATT } 880} \quad (1)$$

232

233 **2.5 Measurement Quality Assurance and Quality Control**

234 It is essential for the data collected in a measurement campaign to have clearly defined provenance.
235 Without descriptions of methodology, stated levels of accuracy, precision, harmonisation and
236 measurement uncertainty, it is extremely difficult to make meaningful comparisons between
237 different datasets and research. This was explored in Stacey (2019), where it was clear that,
238 historically, different UFP studies used a range of instrumentation, setups and calibration
239 methodologies, meaning only qualitative comparisons between them was realistically possible.
240 Wiedensohler et al. (2012) and Wiedensohler et al. (2018) emphasize the need for robust quality
241 control and standardised measurement methodologies; the Heathrow study reported here uses
242 quality assurance and quality control procedures that ensure consistency and comparability in UFP
243 data collection between the Heathrow and national network datasets.
244 For measurements of NO_x, PM₁₀, PM_{2.5}, BC and meteorology, the measurements at Heathrow are
245 managed, collected and processed following guidance described in [https://uk-](https://uk-air.defra.gov.uk/assets/documents/reports/cat09/1902040953_All_Networks_QAQC_Document_2012_Issue2.pdf)
246 [air.defra.gov.uk/assets/documents/reports/cat09/1902040953_All_Networks_QAQC_Document_20](https://uk-air.defra.gov.uk/assets/documents/reports/cat09/1902040953_All_Networks_QAQC_Document_2012_Issue2.pdf)
247 [12_Issue2.pdf](https://uk-air.defra.gov.uk/assets/documents/reports/cat09/1902040953_All_Networks_QAQC_Document_2012_Issue2.pdf). Information about the analysers used at Heathrow is provided in the Supplemental
248 Information, Tables S1 and S2.

249

250 **3. RESULTS**

251 **3.1 Overall Summary**

252 Timeseries data for the hourly measurements of particle number concentrations at LHR2 and Oaks
253 Road are presented in Supplemental Information, Figures S1, S2. Measurements of NO_x, PM₁₀,
254 PM_{2.5} and BC are also fully reported (Figures S3 – S8) and accessible through the
255 <http://heathrowairwatch.org.uk> webpages. Data from these analysers will be used to explore
256 associations and differences to typical ambient environments, but not considered in detail.

257

258

259

260 Measurement data for LHR2 and Oaks Road are summarised in Tables 1 and 2 respectively.

Pollutant	Mean	Median	Standard deviation	Min-Max (15 min data)	Data capture %
NO, ppb	46.9	30.0	56.7	0 – 540	100
NO ₂ , ppb	27.7	27.9	11.7	1 – 84	100
PM ₁₀ , ug/m ³	16.8	12.4	17.2	0.7 – 346.5	100
PM _{2.5} , ug/m ³	10.9	7.2	14.4	0.4 – 288.3	100
BC, ug/m ³	3.11	2.30	2.79	0.08 - 28.08	100
UVPM, ug/m ³	0.84	0.49	0.96	0.03 – 11.41	100
Nucleation, dN/dlog Dp	7817	1871	15993	42 – 150000	87.6
Aitken, dN/dlog Dp	8638	5542	9704	93 – 107918	87.6
Accumulation, dN/dlog Dp	2088	1570	2110	70 – 30052	87.6
Total PN, #/cm ³	8911	4756	12014	394 – 118726	87.6

261 **Table 1.** Summary statistics for measurements at LHR2, 30 Sep to 25 Nov 2016

262
263
264

Pollutant	Mean	Median	Standard deviation	Min-Max (15 min data)	Data capture %
NO, ppb	23.1	10.3	35.1	0 – 328	99.8
NO ₂ , ppb	19.5	19.1	10.3	0 – 68	99.8
PM ₁₀ , ug/m ³	14.3	11.0	12.5	0.8 – 186.6	100
PM _{2.5} , ug/m ³	10.2	6.9	11.1	0.4 – 172.4	100
BC, ug/m ³	1.77	1.20	1.86	0.01 – 26.08	100
UVPM, ug/m ³	0.55	0.37	0.71	0.01 – 6.83	100
Nucleation, dN/dlog Dp	8476	2152	12064	0 – 86287	50.0
Aitken, dN/dlog Dp	7798	4723	8223	0 – 63372	50.0
Accumulation, dN/dlog Dp	1639	1370	1146	0 – 10280	50.0
Total PN, #/cm ³	7408	3948	8180	0 – 62124	50.0

265 **Table 2.** Summary statistics for measurements at Oaks Road, 30 Sep to 25 Nov 2016

266

267 Data for the first week of UFP measurements at LHR2 were rejected due to a software configuration error.

268 Data capture for the UFP analyser at Oaks Road was affected by a software fault with the controlling PC.

269 No data from this analyser was collected after 28 October 2016, data quality for the period 30 Sep to 28 Oct
270 was unaffected by the software fault.

271 As noted earlier, it was not possible to activate remote operation of the analysers by telemetry for this

272 survey. As a result, any instrumental faults arising during the campaign were assessed and corrected during

273 weekly calibration visits to the stations.

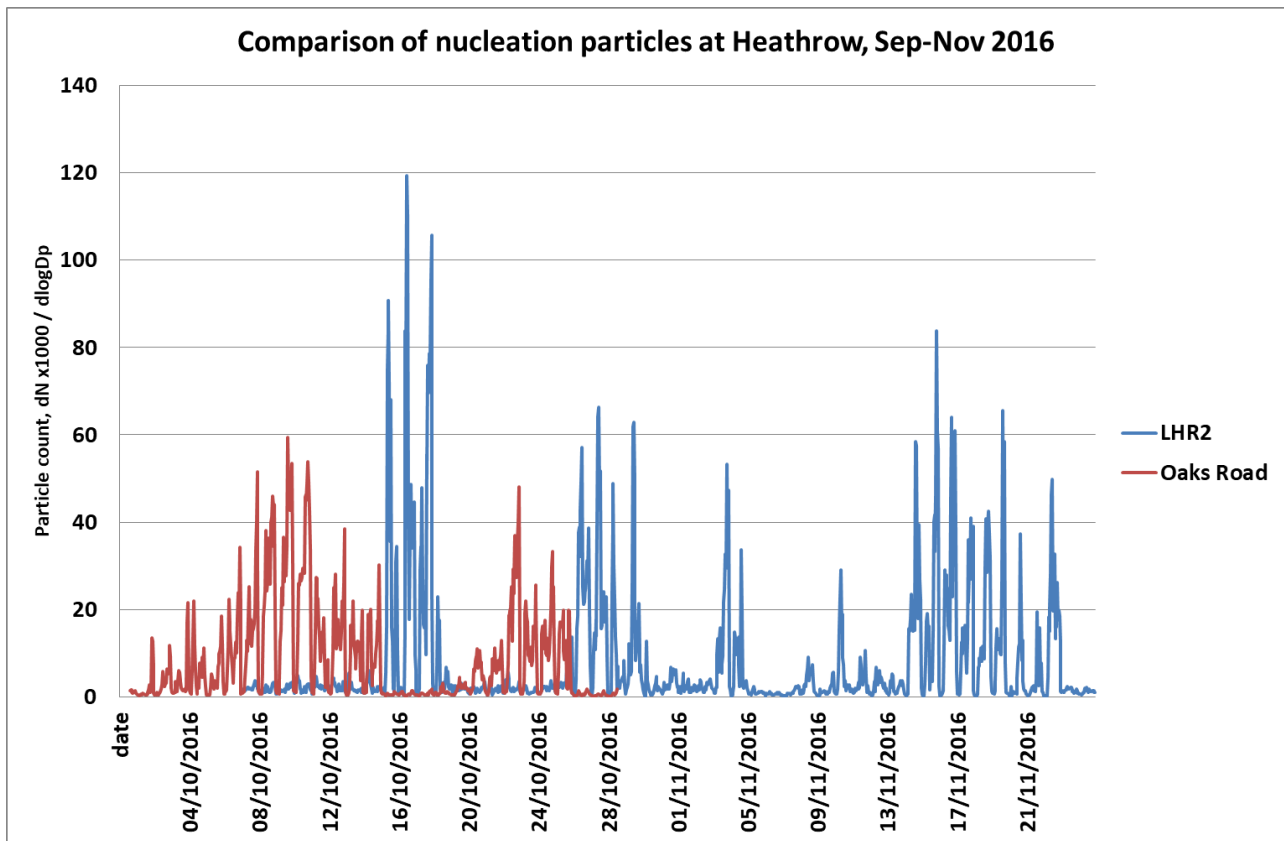
274

275 Examination of historic NO_x, PM and BC data at LHR2 and Oaks Road (available from
276 <http://www.heathrowairwatch.org.uk/reports>) has shown that measured concentrations and profiles for NO_x,
277 PM mass and black carbon are not significantly different to those measured at nearby background and traffic
278 monitoring stations operated by Local Authorities or the national network stations in London.

279

280 It is clear from the particle number timeseries plots in Figures S1 and S2 that there are distinct periods where
281 hourly average concentrations are significantly elevated from the baseline concentrations but equally periods
282 where the PN hourly average concentrations are comparatively low. Figure 2 explores this for nucleation
283 mode particles.

284



285 **Figure 2.** Time series of nucleation mode particles at the Heathrow Airport sampling sites, October
286 and November 2016
287
288
289

290 It is clear from this plot that high concentrations of nucleation mode particles are only observed at
291 one location at a time, so wind direction is a critical factor in the presence and concentration of
292 these particles.

293

294 Examination of LHR2 and Oaks Road particle number diurnal data averaged for the entire survey
295 (presented in Figure S9 and S10) shows enhanced PN concentrations between 06:00 and 23:00,
296 coinciding with typical increased activity around the airport. The diurnal plots also show close
297 agreement with the two humped diurnal profiles of the NO_x and BC pollutants, suggesting that
298 these pollutants mostly share common sources, including road traffic and commercial / domestic
299 energy use. The PM₁₀, PM_{2.5} and accumulation mode particle diurnal plots do not follow the exact
300 same pattern as NO_x, so likely originate from different sources to NO_x. The accumulation mode PN
301 appears to follow a similar trend to the PM₁₀ and PM_{2.5} diurnal profiles, but it is relatively flat and
302 significantly lower in number concentrations when compared to the Nucleation and Aitken mode
303 PN datasets. The diurnal plots for Nucleation and Aitken mode particles do not follow the trends
304 for the other pollutants, further confirming that they are not associated with the same sources.

305

306 **3.2 Results in Context with Other Monitoring Data**

307 Measurements of UFP were coincident at LHR2 and Oaks Road for the period 7 – 28th October
308 2016. As noted earlier, there are three measurement stations within the UK national monitoring
309 network (<https://uk-air.defra.gov.uk/interactive-map>) that measure UFP – these stations were also
310 all in operation during this time. A summary of average concentrations measured at all 5 sites is
311 presented in Table 3.

312

Pollutant	Marylebone Road	North Kensington	Chilbolton	LHR2	Oaks Road
NO, ppb	80.4	9.1	1.6	43.9	21.8
NO ₂ , ppb	39.2	18.9	8.4	27.5	20.7
PM ₁₀ , ug/m ³	21.6	17.1	13.4	15.9	13.8
PM _{2.5} , ug/m ³	12.8	11.1	7.3	9.5	9.4
BC, ug/m ³	3.787	0.912	0.620	2.901	1.792

UVPM, ug/m ³	0.305	0.198	0.277	0.615	0.537
Total PN, particles/cm ³	10046	5384	2637	9053	7964

Table 3. Average pollutant concentrations at Heathrow and comparison stations, 7-28 Oct 2016

313
314
315

316 In this “averaged” scenario, concentrations for all pollutants near the airport can be seen to be
317 largely in the range of the urban traffic and urban background environments of the two London
318 locations, but substantially higher than the rural Chilbolton location.

319

320 Airport PM₁₀ and PM_{2.5} concentrations are slightly lower than seen in London, but different
321 measurement techniques are deployed, which may account for some of the differences. The
322 Heathrow sites use Fidas 200 analysers, while TEOM1400/FDMS8500 units were deployed at the
323 national network stations. There is ongoing work, in preparation for the UK Environment Agency
324 by Ricardo, Bureau Veritas and Kings’ College London, discussed at a number of seminars, for
325 example
326 [http://www.scottishairquality.scot/assets/documents/reports/9 PM analyser replacement Brian Stacey.pdf](http://www.scottishairquality.scot/assets/documents/reports/9_PM_analyser_replacement_Brian_Stacey.pdf),
327 that suggests that there are differences in instrument signal performance that accounts for
328 most of the observed differences in concentrations. This work highlights that detailed knowledge of
329 the operation and limitations of notionally similar measurement devices is essential before drawing
330 any conclusions about observed differences.

331

332 Higher concentrations of UVPM were measured at the airport stations, compared to the London
333 stations. They are likely to be real, although there are again differences in equipment used. The
334 airports use modern AE33-7 seven wavelength aethalometers, while the national network uses older
335 AE22-2 two wavelength instruments. It is possible that differences in attenuation correction
336 protocols (automatically corrected in the AE33, manually corrected post-collection for the AE22),
337 may account for a significant proportion of the differences in measurements. For example, studies
338 undertaken at University of Birmingham (yet to be published), comparing attenuation correction

339 protocols for the AE22 aethalometer published by Virkkula et al (2007) and Apte et al (2011) have
340 found that significant differences in "corrected" concentrations are observed. It can therefore be
341 justifiably argued that neither method for attenuation correction can be guaranteed to give data
342 comparable to that produced by the AE33 aethalometer, where no correction for attenuation is
343 required.

344

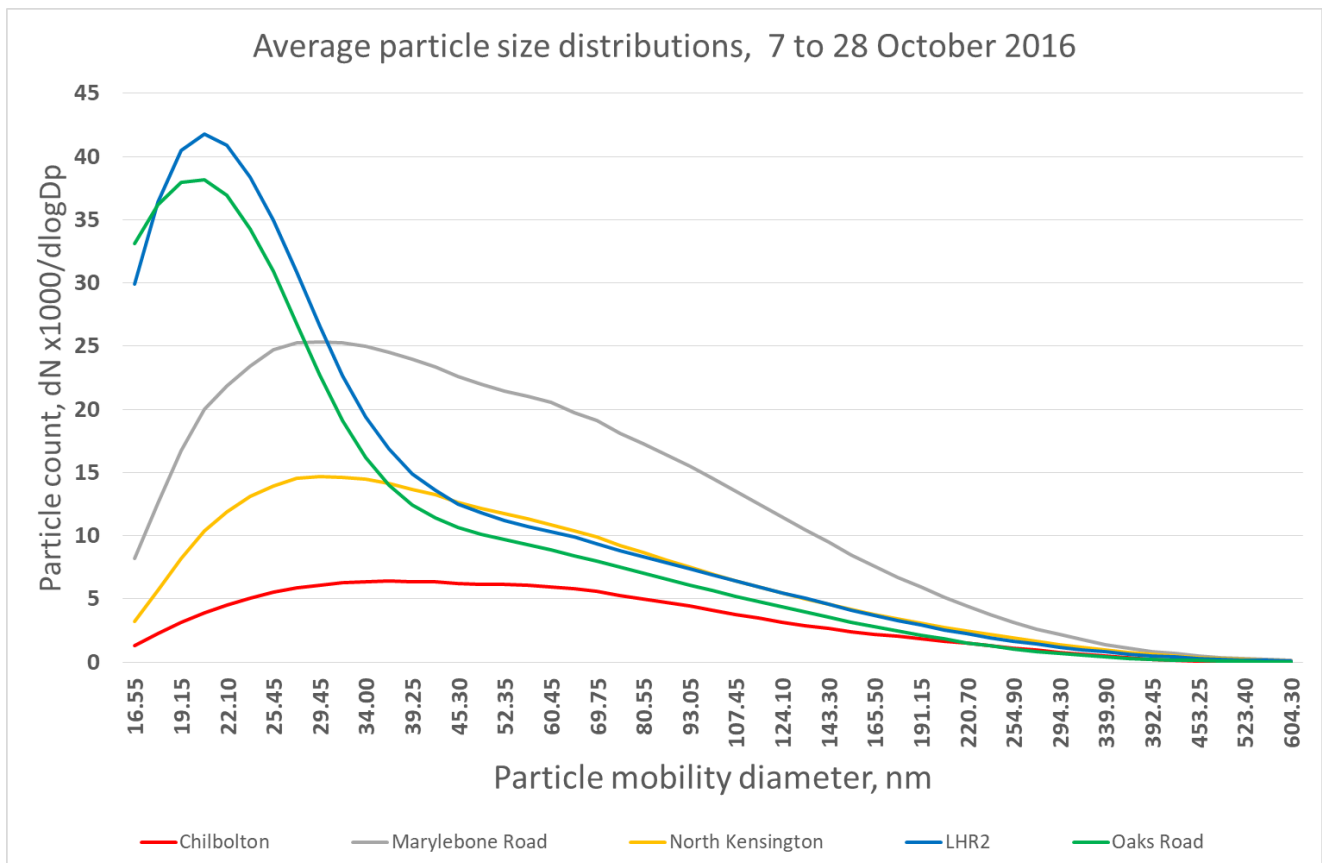
345 Averaged particle number concentrations, calculated by summing all of the particle counts from the
346 SMPS analysers from 14.6nm to 661.2nm, shows that a similar trend is observed to other
347 pollutants: concentrations at the airport locations fall between the traffic and background
348 measurements made at the London stations.

349

350 On initial investigation of the measurement datasets therefore, the ambient air environment at
351 Heathrow appears reasonably similar to the rest of London. However, data from the SMPS
352 analysers also provides valuable information about the particle size distribution at all 5 locations. It
353 has already been demonstrated in earlier research that nucleation mode particles are strongly
354 associated with airport activity. The plot in Figure 3 shows the average particle size distribution at
355 each station for the period when all 5 SMPS were operational; the period between 7 and 28th
356 October 2016.

357

358



359
360 **Figure 3.** Comparison of particle size distributions at 5 locations
361
362

363 There are many points that are striking about this data:

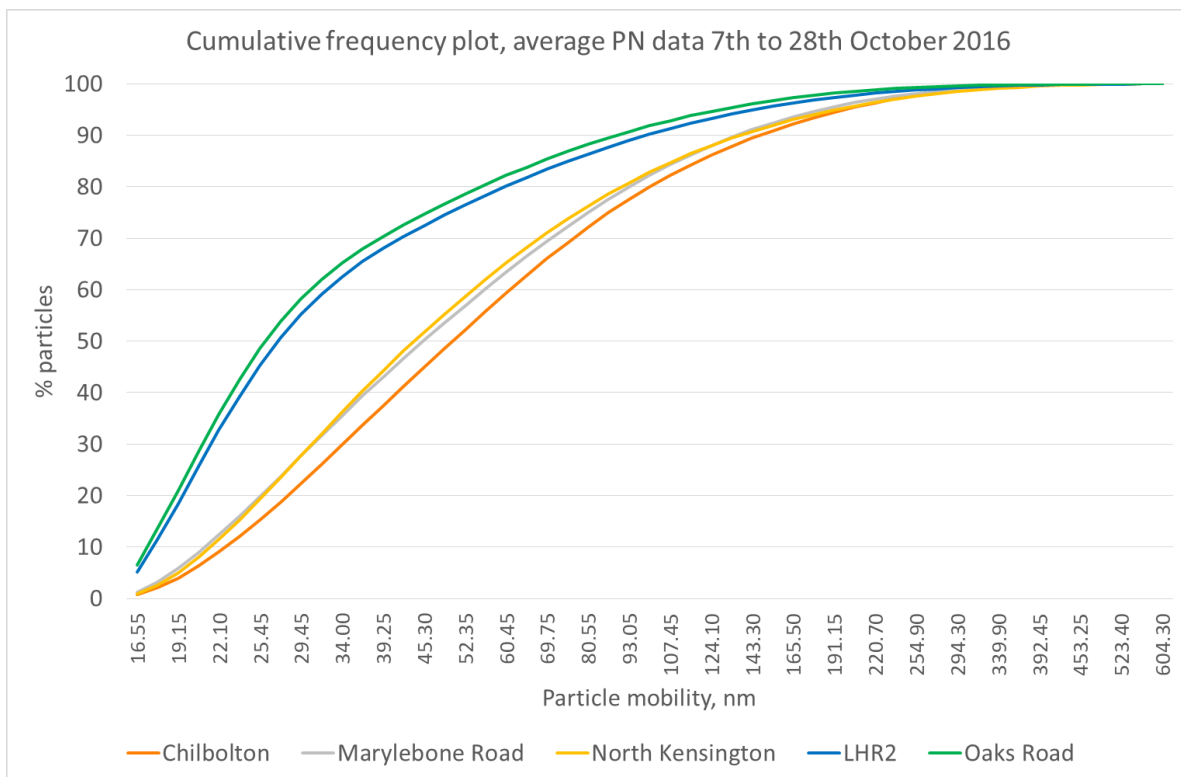
- 364 • The size distributions for Marylebone Road and North Kensington are remarkably similar,
365 differing only in magnitude. The mode value for both stations is ~30nm, suggesting that both
366 stations share commonality of source origins.
- 367 • Chilbolton concentrations are much lower, with a larger mode particle size value of ~37nm.
368 The distribution profile is otherwise reasonably similar to the London stations.
- 369 • For particle sizes larger than ~40nm, the LHR2 profile follows a very similar profile to the
370 North Kensington station
- 371 • The Oaks Road particle distribution profile is very similar to LHR2 for particles up to about
372 150nm in size. For particles larger than 200nm, Oaks Road follows a profile similar to
373 Chilbolton, suggesting that these larger particles are more background in nature than the
374 LHR2 station.

375

376 The most obvious observation about the airport particle size distribution (PSD) is how the particle
 377 number concentrations smaller than 40nm differ significantly from the other three datasets. The
 378 mode value for LHR2 and Oaks Road is ~20nm, significantly smaller particle modes than at the
 379 other 3 stations. It is clear from this plot that the ambient environment close to the airport is
 380 significantly different for smallest particle numbers compared to typical urban environments.

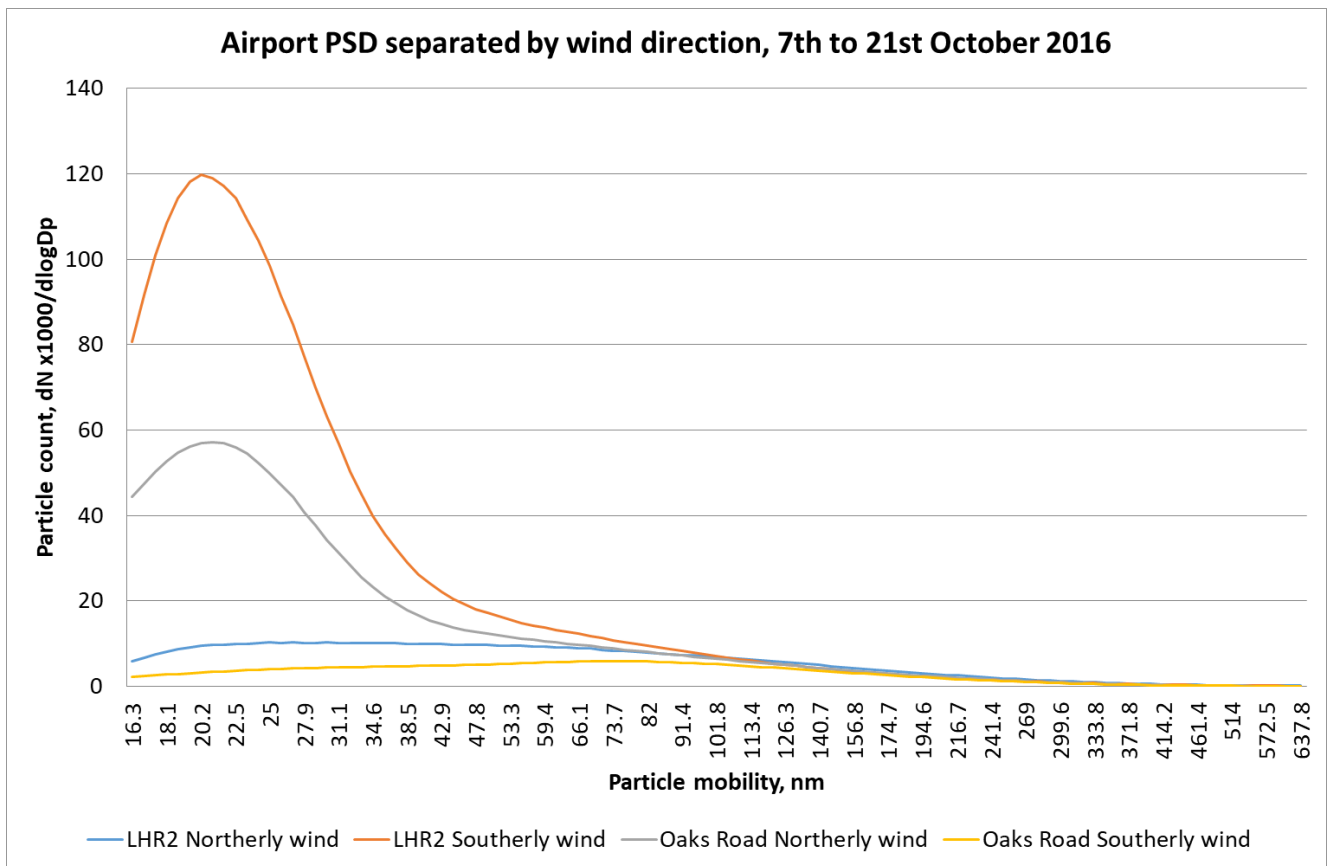
381
 382 The data are further analysed using a cumulative frequency plot, which sums the proportion of total
 383 particles within the increasing particle size dataset. The CFD plot in Figure 4 for all 5 locations
 384 supports the observation in Figure 3 that most particles at the airport are smaller in nature than in
 385 typical urban environments. At Marylebone Road and North Kensington, 50% of the particles are
 386 smaller than ~50nm, whereas at LHR2 and Oaks Road, 50% of all particles are smaller than ~25nm,
 387 suggesting a distinct and different source near the airport.

388
 389



390
 391 **Figure 4.** Cumulative particle size distributions at the five sites.
 392

393 The directional nature of the UFP emissions can be explored further by looking at PSD at LHR2
 394 and Oaks Road when winds are split into roughly northerly (the wind segment clockwise from 270
 395 to 90 degrees) and southerly (clockwise from 90 to 270 degrees) segments. Figure 6 explores these
 396 data.
 397



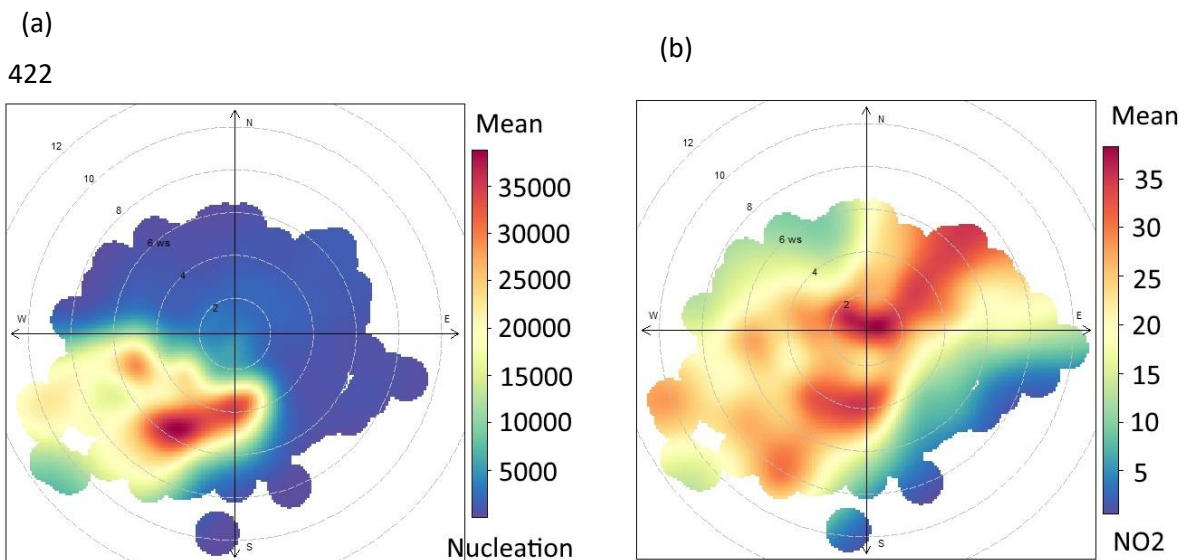
398 **Figure 6.** Airport PSD separated by wind direction for the Heathrow Airport sites. Note that the
 399 particle mobility axis differs slightly from earlier figures due to the need to align Heathrow particle
 400 size concentrations exactly with the data provided by the national network stations.
 401
 402
 403

404 This plot clearly shows that when the wind does not originate from the airport (Northerly for LHR2
 405 and Southerly for Oaks Road), the PSD profile of measurements is broadly similar to measurements
 406 made at the London urban locations. In contrast, when the stations are directly impacted by winds
 407 from the airport, the PSD profiles are dominated by very fine particles. LHR2, which is just 170m
 408 from the runway and unobstructed by buildings and other infrastructure, experiences much higher
 409 average particle counts than Oaks Road, over 600m from the runway and surrounded by residential
 410 buildings.

411
412
413
414
415
416
417
418
419

3.3 Dependence of Airport Measurements on Meteorology

Meteorological measurements made at Heathrow allow for further analysis of the data using the polarPlot function in OpenAir. The plots in Figure 7 examine the dependence of measurements on wind speed and direction.



423
424
425
426

Figure 7. Polar plots for LHR2 data, (a) nucleation mode particles, (b) nitrogen dioxide

427 The plots for nucleation mode (Figure 7(a)) and Aitken mode (Figure S11) mode particles show a
428 very strong influence from the airport, to the south and west of the measurement station. The
429 nucleation mode particles plot shows very little influence from other directions, clearly pointing to
430 airport activities as the dominating source of these particles at this location.

431

432 NO₂ at LHR2 (Figure 7(b)) is strongly associated with south west and north east wind directions,
433 but also to a lesser extent from other directions. This reflects the multiple source nature of NO₂ in

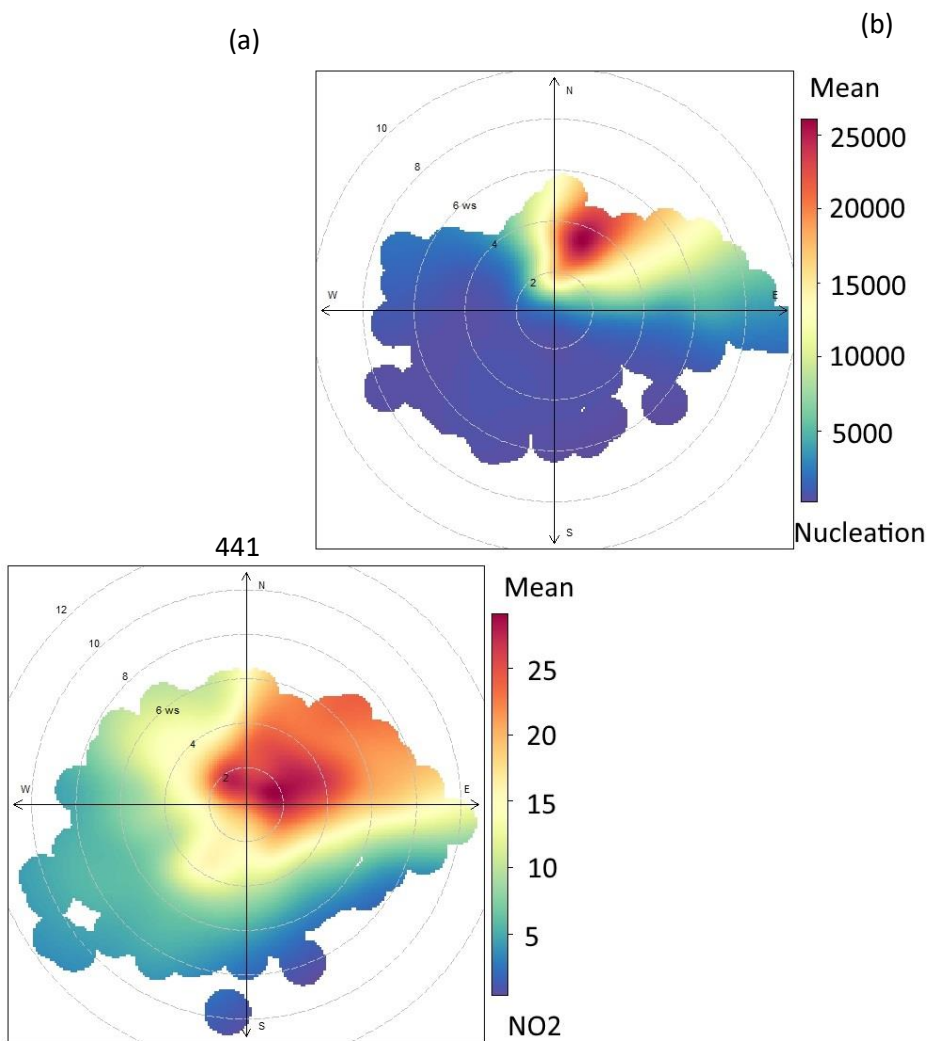
434 the environment; road traffic and domestic / commercial energy use from many sources around the
435 station are all seen to influence the polar plot.

436

437 NO, BC, UVPM and accumulation mode particles (presented in Figure S11) are associated with
438 most wind directions and also at low wind speeds.

439 Similar patterns are seen at Oaks Road (Figure 8).

440



442

443

444 **Figure 8.** Polar plots for Oaks Road, (a) nucleation mode particles, (b) nitrogen dioxide

445

446

447 The plots show that high concentrations of nucleation mode particles, as well as NO₂, are strongly

448 associated with winds from the airport. Aitken mode particles (in Figure S12) follow a similar

449 trend to nucleation mode particles, but are associated with a slightly wider range of wind directions
450 than the nucleation mode. It is clear from the two monitoring station datasets that nucleation mode
451 particles are predominantly associated with winds from the airport, suggesting that the airport is by
452 far the major source of emissions of these particles.

453

454 In contrast, all other pollutants (Figure S12) are strongly influenced by low wind speeds, indicating
455 local sources, and the background environment as significant contributors. PM₁₀ and PM_{2.5} appear
456 to originate largely from the same common sources, and PM mass sources appear to be mostly
457 independent from the other pollutants.

458

459 **3.4 Dependence of Measurements on Airport Operation**

460 The two runway configuration at Heathrow allows the airport to operate in a number of modes.

461 When winds are easterly, aircraft exclusively depart from Runway 09R, the southernmost runway,
462 and generally arrive on 09L, the northerly runway.

463

464 When winds are westerly, the airport typically operates a shift-based departure system, departing on
465 one runway for half the day, and the other runway for the remainder. Landing occurs on the other
466 runway during these times.

467

468 These operating modes are primarily chosen for practicality. For westerly departures, spreading the
469 distribution of landings and departures on Runways 27R and 27L equalises the wear and tear on the
470 landing zones on each runway, reducing the amount of maintenance required. For easterly
471 departures, the taxiways approaching the thresholds of Runway 09L are not suitable for modern
472 aircraft. This means that departures in this mode are exclusively from Runway 09R.

473

474 The airport is typically closed to most air traffic during the hours 23:00 to 05:00 local time.

475

476 Access to aircraft arrival and departure information, provided by Heathrow Airport Limited, allows
477 the measurement data to be examined in far greater detail. The three modes, departing from 09R,
478 27L and 27R, plus the overnight period, are presented as polar plots for nucleation mode particles in
479 Figure 9.

480

481

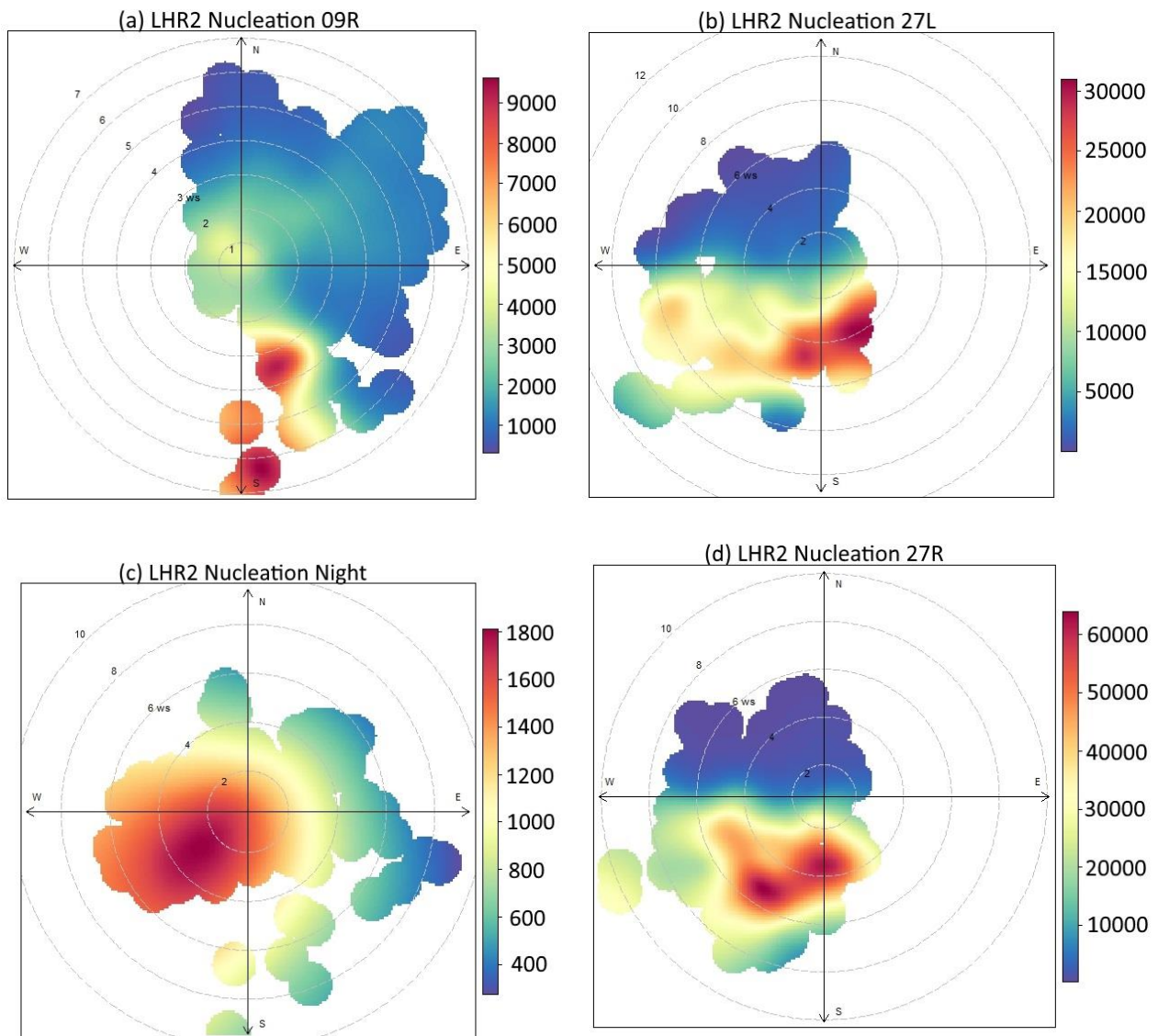
482

483

484

485

486



487

488

489

490 **Figure 9.** Polar plots of nucleation mode particles at LHR2, split by runway mode, (a) 09R, (b) 27L, (c)
491 Night, (d) 27R. Each sub plot has different maximum concentrations defining the colour scales.

492
493
494 It is clear that nucleation mode particle number concentrations are highest when aircraft depart from
495 27R (closest to the monitoring station) and lowest when the airport is closed overnight. Nucleation
496 particle numbers are significantly higher when aircraft are departing on 27R compared to when they
497 are landing on 27R (departing on 27L) Even when aircraft are departing from 09R, a small yet
498 clear peak in nucleation mode particles can still be seen from the airfield, presumably from
499 departing aircraft exhaust – arriving aircraft leave the runway before they are within 1km of the
500 LHR2 monitoring station and are thus not expected to significantly influence measurements during
501 easterly winds. Overnight concentrations of nucleation particles are generally comparatively very
502 low, but still appear to be associated with winds from the airfield.

503

504 The plots for Aitken mode particles for 27R and 27L are very similar to those seen for nucleation
505 mode particles (presented in Figure S13), suggesting that the largest influence for these particles
506 still comes from the aircraft. In contrast, the polar plots for Aitken mode particles from 09R and
507 overnight (presented in Figure S13) differ from the nucleation mode plots, being both significantly
508 lower in concentration and showing more influence from lower wind speed meteorology. This
509 suggests more diverse source origins than just the dominance of the airport in nucleation mode
510 measurements.

511

512 The polar plots (presented in Figure S14) for black carbon, measured by the Aethalometer, illustrate
513 that BC is neither strongly associated with airport activity or nucleation mode particles. This
514 reinforces work conducted by Costabile et al. (2015), which found no strong links between aircraft
515 emissions and elevated BC measurements.

516

517 The polar plots (presented in Figure S14) for UVPM, measured by the Aethalometer, suggest that
518 elevated concentrations of UVPM at LHR2 might have an association with nucleation mode

519 particles when aircraft are departing from runway 27R. A similar link is not obvious when aircraft
520 are landing on 27R, 09R or indeed any other aircraft operating modes at the airport, suggesting that
521 high thrust exhaust emissions may be associated with production of black carbon particles that
522 strongly attenuate UV light. In contrast (in Figure S15), UVPM at Oaks Road is dominated by
523 association with low wind speeds. There is some indication of a contribution from the direction of
524 the airport, but it is likely that a number of different sources contribute to measurements in this
525 residential location.

526

527 For Oaks Road, a similar picture emerges (plots presented in Figure S15). Highest concentrations
528 of nucleation mode particles are associated with aircraft departing from 09R, closest to the
529 monitoring station, but high concentrations of nucleation mode particles in other polar plot modes
530 clearly also originate from the airfield.

531

532 Polar annuli for all pollutants at both sites are presented in Figures S16 and S17. These plots
533 further reinforce the directional and diurnal nature of emissions around the airport

534

535 **3.5 Examination of Fine Temporal Resolution Data**

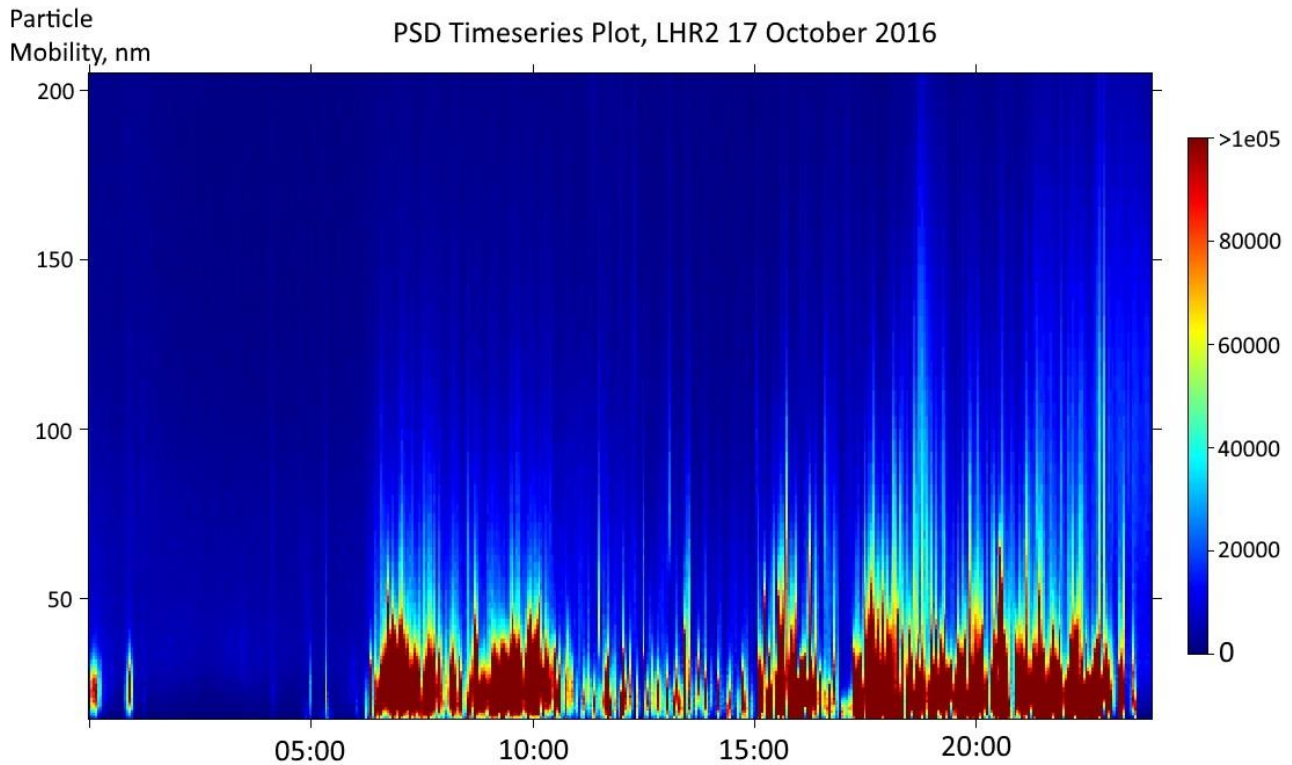
536 The monitoring station at LHR2 is 170m from the centre of the northern runway. Under favourable
537 meteorology, plumes from aircraft departing and landing impact on the monitoring station, raising
538 the possibility that these plumes can be further analysed and characterised by, for example, aircraft
539 type, engine type, aircraft landing and aircraft departing.

540

541 On average ([https://www.heathrow.com/file_source/Company/Static/PDF/Investorcentre/Heathrow-
542 \(SP\)-FY2016-results-release-\(FINAL\).pdf](https://www.heathrow.com/file_source/Company/Static/PDF/Investorcentre/Heathrow-
542 (SP)-FY2016-results-release-(FINAL).pdf)), an aircraft departs from the airport every 90 seconds
543 between 06:00 and 23:00 every day. The SMPS/CPC configuration at LHR2 was set to provide a
544 full particle size sweep every three minutes, meaning that it was impossible (with this dataset) to

545 uniquely assign a single measurement to an individual aircraft. Nevertheless, some structure in the
546 PN measurements can be observed which bears excellent correlation to the runway operations. The
547 plot in Figure 10 presents a timeseries of PSD collected on 17 October.

548
549



550 **Figure 10.** Particle Size Distribution plot, LHR2, 17 October
551

552
553

554 The plot shows that the smallest particles have the highest concentrations, and a clear temporal
555 correlation to airport activity (from around 6am to 11pm). Particle number concentrations are very
556 low between midnight and 06:00. Aircraft movement information obtained from the airport for 17
557 October confirmed that aircraft departed from 27R (closest to the station), between the hours of
558 06:00 and 10:00, and 15:00 to 23:00. Aircraft landed on 27R between 10:00 and 15:00. This
559 information supports the observations in Figure 6: PN concentrations are clearly lower between
560 10:00 and 15:00, suggesting that emissions of nucleation mode particles from landing aircraft are
561 significantly lower than those from departing aircraft. This observation was repeated throughout
562 the survey, though the meteorology made this most obvious on 17th October.

563

564 As was seen in Figure 9, the activities on the southern runway have an effect on measured
565 concentrations at LHR2, so it is likely that the departing aircraft on the southerly runway 27L will
566 also have an impact, albeit much less than the northern runway, on the measurements at LHR2.
567 However, it is not possible to decouple these emissions from the landing aircraft on 27R to
568 investigate this, and it assumed that, at least for aircraft departing on 27R, any contribution from
569 emissions on 27L is overwhelmed by the proximity of the nearest emissions.

570

571 **3.6 Comparison with Receptor Modelling Outputs**

572 Masiol et al. (2017) undertook a similar study at Heathrow Airport in 2014/15, investigating UFP
573 concentrations at a monitoring station 1km NE of LHR2 (London Harlington, part of the UK
574 national monitoring network). The data collected were analysed using *k*-mean clustering and
575 positive matrix factorisation (PMF), which revealed the contribution of the airfield to local particle
576 number concentrations (high concentrations, mode concentration ~20nm). Masiol et al. (2017)
577 calculated that at the London Harlington station, approximately one third of the total measured PN
578 concentrations originated from the airport.

579

580 Data collected from this 2016 LHR2 and Oaks Road study were analysed using the PMF5 positive
581 matrix factorisation source apportionment model (v5.0.14.21735, U.S. Environmental Protection
582 Agency, USA). Details of the model and usage methodologies are comprehensively described by
583 many authors including, for example Rizzo and Scheff (2007), Masiol et al. (2017), and in
584 USEPA's own guidance: [https://www.epa.gov/sites/production/files/2015-
585 02/documents/pmf_5.0_user_guide.pdf](https://www.epa.gov/sites/production/files/2015-02/documents/pmf_5.0_user_guide.pdf) and
586 <https://www3.epa.gov/ttnamti1/files/ambient/pm25/workshop/laymen.pdf>

587

588 For LHR2 and Oaks Road, analysis was focussed on qualitative output. The factors identified by
589 the model were used to compare against the measurement data analysed using the tools in R and
590 OpenAir. No effort has been made at this stage to normalise the extremes of measured
591 concentrations in the model to allow for detailed quantitative assessments.

592

593 In order for the model to run more effectively, SMPS data from both locations was aggregated into
594 hourly means and then further aggregated into a reduced number of size bins – 15, reduced from the
595 107 size fractions natively output by the SMPS in this configuration. The data from the 14.6nm and
596 680nm channels was rejected for this analysis, to remove any possible influence from spurious data
597 at the start and end of the SMPS measurement cycles. Data from the other pollutants at the station:
598 NO, NO₂, NO_x, BC, UVPM, PM₁₀, and PM_{2.5} were also included in the PMF runs.

599

600 Uncertainties and detection limits (DL) for all pollutants were derived from data provided in the
601 Supplementary Information, with the exception of PN, which was set to 100% uncertainty and DL
602 of 100 particles/cm³. Where measurements were lower than the stated detection limit, the DL value
603 was substituted into the uncertainties data. An additional 10% uncertainty was added to the model
604 before all runs.

605

606 The model was run for 3 to 10 factor scenarios, with strong relationships set for all pollutants except
607 PM₁₀ and PM_{2.5}. The total variable was set to total PN (the sum of all PN data from 15-640nm) and
608 assigned strong status. The base model was set to 100 runs, although there was little difference
609 between this solution and a 20 run solution, confirming that both analyses are robust. Displacement
610 analysis was run using default settings. Bootstrapping used default settings for 50 bootstraps. For
611 BS-DISP, all Strong channels except Total PN were enabled for the analysis.

612

613 The model outputs were examined to check that all factors were unique and that factors had not
614 been subdivided unnecessarily. There was no adjustment required for rotational ambiguity.

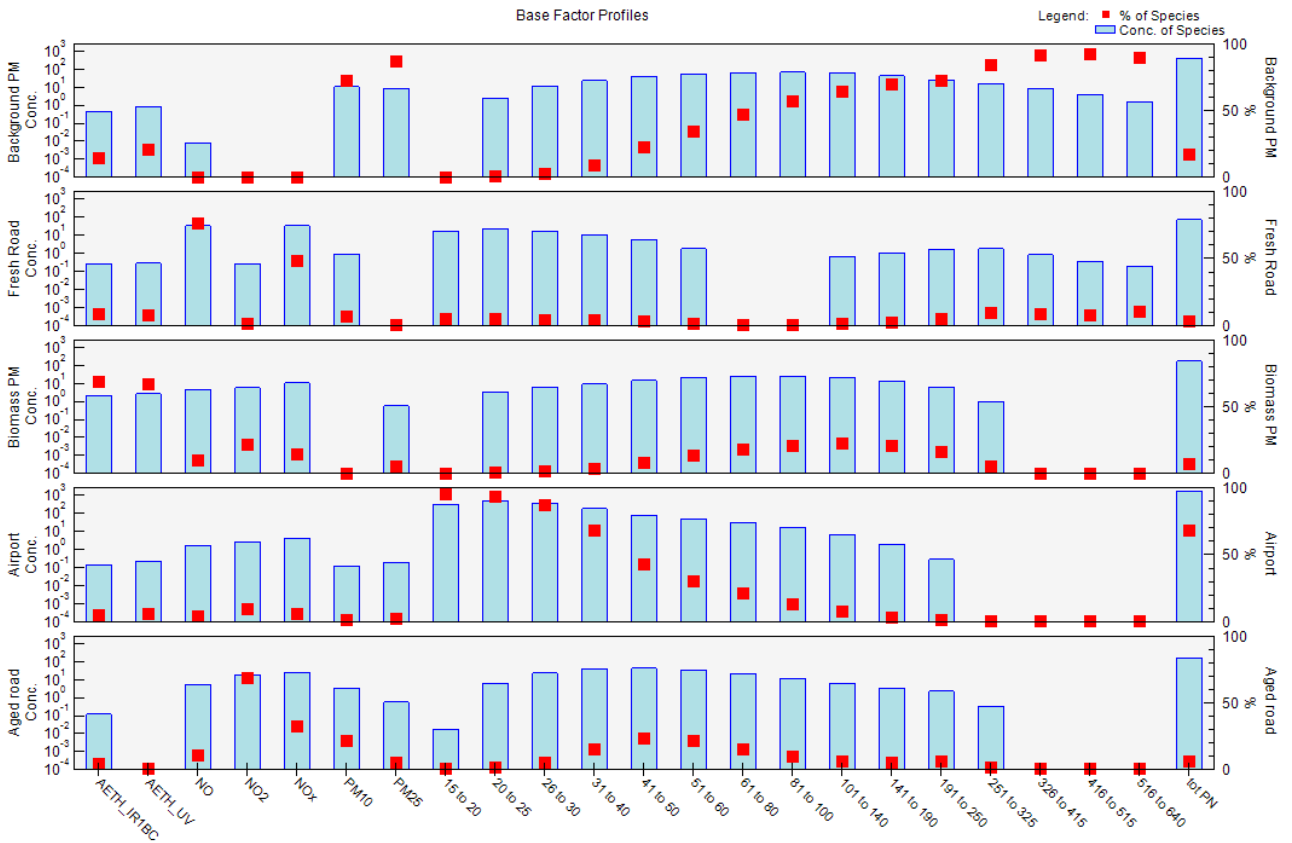
615

616 At both locations, 5 factors was identified as the optimal number, with factors identified as:

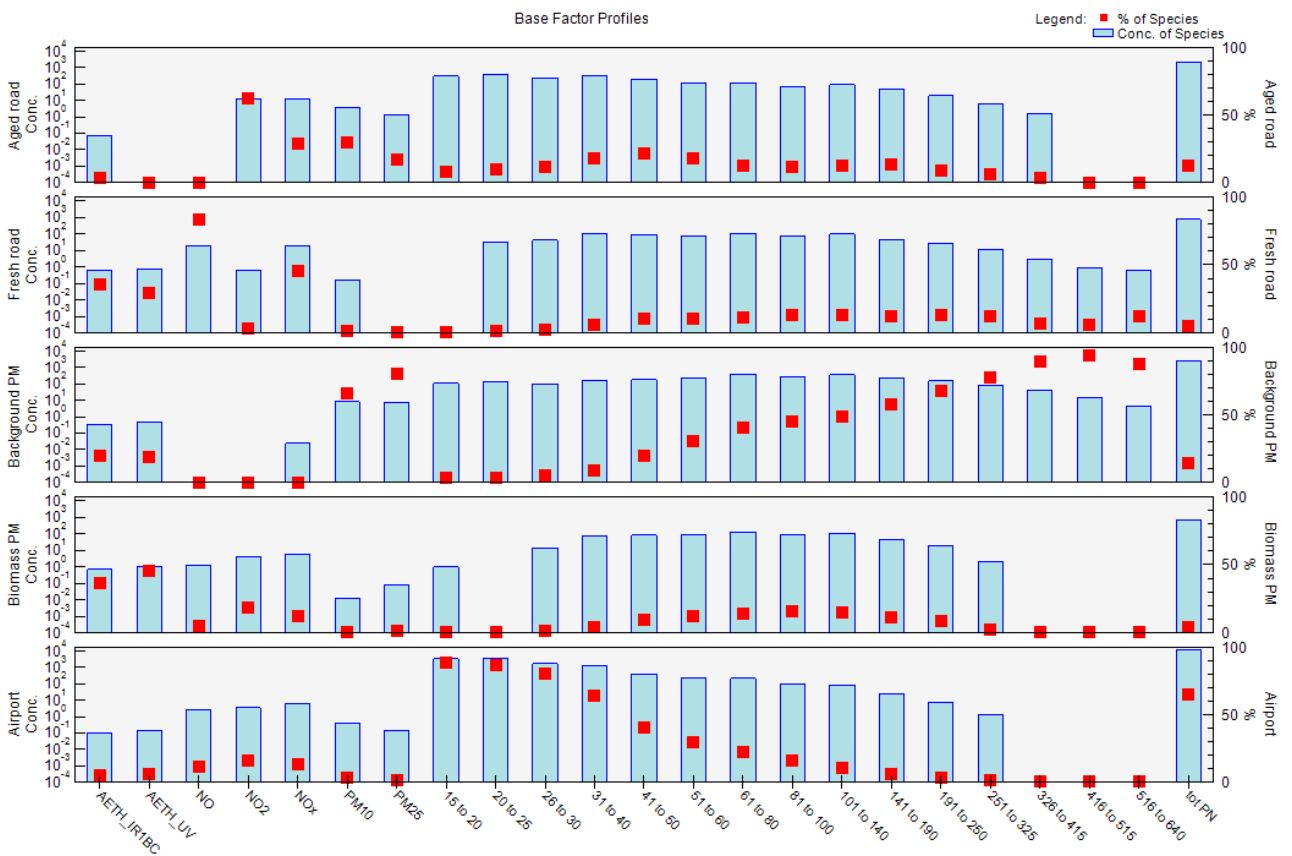
- 617 • Airport. Factor dominated by PN <50nm, comparatively low contribution from all other
618 pollutants.
- 619 • Fresh road traffic. Factor dominated by high concentrations of NO. Minor contribution also
620 from larger particles.
- 621 • Aged road traffic. Factor dominated by NO₂. PN from 30-80nm and PM₁₀ also observed
- 622 • Biomass PM. Factor dominated by BC, UVPM and particles 80 – 250nm. NO_x and PM_{2.5}
623 also observed.
- 624 • Background PM. Factor dominated by PM₁₀, PM_{2.5} and particles 80 – 640nm. BC and UVPM
625 also observed.

626

627 The plots in Figures 11 and 12 show the base factor profiles for LHR2 and Oaks Road, with factors
628 labelled according to identified sources.



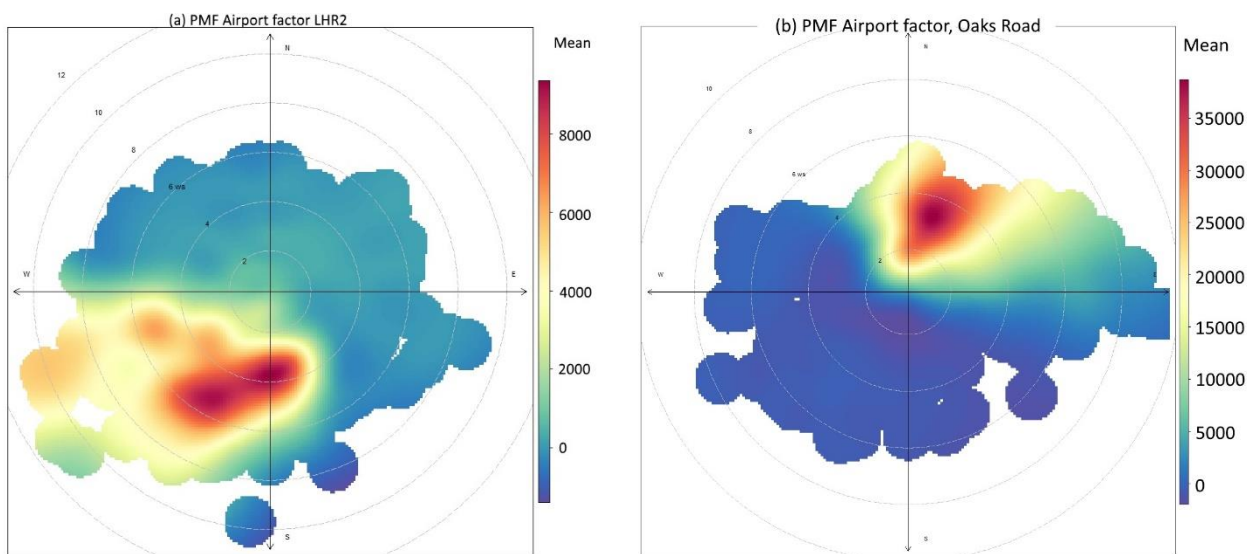
629
630 **Figure 11.** PMF Base Factor Profiles for LHR2 site
631



632
633 **Figure 12.** PMF Base Factor Profiles for the Oaks Road site
634

635
636 The model runs at both stations clearly identify the very fine particles associated with aircraft
637 movements. The Aircraft factor from both LHR2 and Oaks Road models is overwhelmingly
638 dominated by particles in the 15-50nm size range. 93 to 95% of the 15 to 25nm particles measured,
639 and 68% of all particles smaller than 660nm measured at LHR2 originate from the Airport factor
640 (At Oaks Road, these figures are 86 to 89% and 65% respectively). The factor explains very little of
641 the variation in NO_x, BC or PM however, suggesting that other sources dominate the contribution to
642 local air quality. All iterations of the model runs from 3 to 10 factors were successful in separating
643 this factor and its profile at both locations, further supporting the clear aircraft contributions at the
644 stations.
645 To add further confidence that the PMF model was extracting the airport factor consistently at both
646 LHR2 and Oaks Road, factor data for each factor run were input into regression analysis with
647 different factor scenarios. The results of these regressions showed extremely high correlation
648 between the different factor runs and are presented in Figures S20 to S23.

649
650
651
652
653
654



655
656 **Figure 13.** Polar plots of Aircraft PMF factors at (a) LHR2 and (b) Oaks Road
657
658

659 Analysis of the extracted aircraft factors from LHR2 and Oaks Road when combined with the
660 meteorological data from LHR2 in polar plots shows the airport source very clearly in Figure 13 (to
661 the south west at LHR2 and north east at Oaks Road) and compare exceptionally well to the polar
662 plots for measured nucleation particles presented in Figures 7 and 8. This further confirms the
663 robust analysis of the measurement data and the role of aircraft in the concentrations of the finest
664 particle sizes measured near Heathrow Airport.

665

666 As a further data quality check, the model was run at LHR2 and Oaks Road with all SMPS channels
667 retained in the model run unaggregated. The base model plots are presented in Figures S18 and S19
668 and confirm that the qualitative accuracy of splitting out the factors is unaffected by aggregating the
669 PN size bins.

670

671

672 **4. CONCLUSIONS**

673 An extensive campaign to monitor UFP at Heathrow was undertaken in the autumn of 2016. The
674 objective was to assess the context of measurements at the airport compared to measurements at
675 “typical” traffic, background and rural locations in the south east of England.

676

677 Monitoring at the two locations at the airport was configured to ensure direct comparability with
678 other measurements made in south east England.

679

680 Average concentrations at the airport, taking no account of particle size distributions, showed that
681 total particle number concentrations the airport fits within the range of traffic and urban background
682 locations in London, matching the trends seen for NO_x , PM_{10} , $\text{PM}_{2.5}$ and BC. The distribution of
683 particle sizes is however, completely different, with the airport PSD dominated by particles with a
684 mode of 20nm. In contrast, measurements of PN in London have a significantly larger mode of
685 30nm. We believe that this is the first time this type of concurrent comparison of airport and urban
686 UFP has been undertaken, providing valuable insight into the nature of the different environments.

687

688 Further investigation of the nucleation mode particles and meteorology reveals that measurements
689 of particle number from within the airport perimeter are dominated by these smallest particles and
690 are closely associated with aircraft. Analysis of the operating modes at the airport showed that
691 aircraft departing from the airport emit particles in much higher numbers than those arriving.

692

693 Nucleation mode particles from the airport are not strongly associated with Black Carbon, though,
694 at LHR2, there does appear to be some correlation with BC particles that strongly absorb UV light.
695 There is a modest association between nucleation mode particles and NO_2 .

696

697 The Heathrow data were analysed using the USEPA PMF model to separate the contributions into 4
698 factors. A clear airport component was identified at both locations, where the largest proportion of
699 the factor was associated with nucleation mode particles. Examination of these factor datasets in
700 polar plots showed excellent agreement with the nucleation mode polar plots using data collected
701 from the analysers.

702

703

704 **DATA AVAILABILITY**

705 Data supporting this publication are openly available from the UBIRA eData repository at
706 <https://doi.org/10.25500/edata.bham.00000349>.

707

708 **ACKNOWLEDGEMENTS**

709 The authors gratefully acknowledge Heathrow Airport Limited for sponsoring this doctoral research
710 project.

711

712

713 **REFERENCES**

- 714 Abegglen, M., Brem, B.T., Ellenrieder, M., Durdina, L., Rindlisbacher, T., Wang, J., Lohmann, U.
715 and Sierau, B., 2016. Chemical characterization of freshly emitted particulate matter from aircraft
716 exhaust using single particle mass spectrometry, *Atmos. Environ.*, 134, 181-197,
717 <http://dx.doi.org/10.1016/j.atmosenv.2016.03.051>
718
- 719 Apte, J.S., Kirchstetter T.W., Reich, A.H., Deshpande, S.J., Kaushik, G., Chel, A., Marshall, J.D.
720 and Nazaroff, W.W., 2011. Concentrations of fine, ultrafine, and black carbon particles in auto-
721 rickshaws in New Delhi, India, *Atmos. Environ.*, 45, 4470-4480.
722
- 723 Beyersdorf, A.J., Timko, M.T., Ziemba, L.D., Bulzan, D., Corporan, E., Herndon, S.C., Howard,
724 R., Miake-Lye, R., Thornhill, K.L., Winstead, E., Wey, C., Yu, Z. and Anderson, B.E., 2014.
725 Reductions in aircraft particulate emissions due to the use of Fischer–Tropsch fuels, *Atmos. Chem.*
726 *Phys.*, 14, 11-23, <https://dx.doi.org/10.5194/acp-14-11-2014>
727
- 728 Bezemer, A., Wesseling, J., Cassee, F., Fischer, P., Fokkens, P., Houthuijs, D., Jimmink, B., de
729 Leeuw, F., Kos, G., Weijers, E., Keuken, M. and H. Erbrink, 2015. Nader verkennend onderzoek
730 ultrafijnstof rond Schiphol, RIVM Rapport 2015-0110,
731 <https://zembla.bnnvara.nl/data/files/1851392849.pdf>
732
- 733 Carslaw, D.C. and Ropkins, K., 2012. *openair* – An R package for air quality data analysis,
734 *Environmental Modelling and Software*, *Environ. Model. & Softw.*, 27-28, 52-61,
735 <https://dx.doi.org/10.1016/j.envsoft.2011.09.008>
736
- 737 Costabile, F., Angelini, F., Barnaba, F. and Gobbi, G.P., 2015. Partitioning of black carbon
738 between ultrafine and fine particle modes in an urban airport vs. urban background environment,
739 *Atmos. Environ.*, 102, 136-144, <http://dx.doi.org/10.1016/j.atmosenv.2014.11.064>
740
- 741 Donaldson, K., Stone, V., Clouter, A., Renwick, L. and MacNee, W., 2001. Ultrafine particles,
742 *Occup. Environ. Med.*, 58, 211-216, <https://dx.doi.org/10.1136/oem.58.3.211>
743
- 744 Durdina, L., Brem, B.T., Abegglen, M., Lobo, P., Rindlisbacher, T., Thomson, K.A., Smallwood,
745 G.J., Hagen, D.E., Sierau, B. and Wang, J., 2014. Determination of PM mass emissions from an
746 aircraft turbine engine using particle effective density, *Atmos. Environ.*, 99, 500-507,
747 <http://dx.doi.org/10.1016/j.atmosenv.2014.10.018>
748
- 749 Ellermann, T., Massling, A., Løfstrøm, P., Winther, M., Nøjgaard, J.K. and Ketzel, M., 2012.
750 Assessment of the air quality at the apron of Copenhagen Airport Kastrup in relation to the
751 occupational environment, Aarhus University, DCE - Danish Centre for Environment and Energy,
752 51pp. - Technical report from DCE – Danish Centre for Environment and Energy No. 15.,
753 <http://www2.dmu.dk/Pub/TR15.pdf>
754
- 755 Ellermann, T., Massling, A., Løfstrøm, P., Winther, M., Nøjgaard, J.K. and Ketzel, M., 2011.
756 Undersøgelse af luftforureningen på forpladsen i Københavns Lufthavn Kastrup i relation til
757 arbejdsmiljø. DCE - Nationalt Center for Miljø og Energi, Aarhus Universitet. 148 s. - Teknisk
758 rapport fra DCE – Nationalt Center for Miljø og Energi nr. 5, <http://www2.dmu.dk/Pub/TR5.pdf>
759
- 760 Fanning, E., Yu, R.C., Lu, R. and Froines, J., 2007. Monitoring and modeling of ultrafine particles
761 and black carbon at the Los Angeles International Airport, ARB contract number 04-325,
762 <https://ww3.arb.ca.gov/research/apr/past/04-325.pdf>
763

764 Fleuti, E., Maraini, S., Bieri, L. and Fierz, M., Ultrafine Particle Measurements at Zurich Airport,
765 University of Applied Sciences and Arts Northwestern Switzerland FHNW,
766 [file:///C:/Users/hardinmt/Downloads/2017-03_Zurich-Airport_UFP_Study%20\(1\).pdf](file:///C:/Users/hardinmt/Downloads/2017-03_Zurich-Airport_UFP_Study%20(1).pdf)
767 Health Effects Institute, 2013. HEI Review Panel on Ultrafine Particles. Understanding the Health
768 Effects of Ambient Ultrafine Particles, HEI Perspectives 3, Health Effects Institute, Boston MA.
769 <https://www.healtheffects.org/system/files/Perspectives3.pdf>
770
771 Hudda, N. and Fruin, S.A., 2016. International airport impacts to air quality: Size and related
772 properties of large increases in ultrafine particle number concentrations, Environ. Sci. Technol., 50,
773 3362-3370, <https://dx.doi.org/10.1021/acs.est.5b05313>
774
775 Keuken, M.P., Moerman, M., Zandveld, P., Henzing, J.S. and Hoek, G., 2015. Total and size-
776 resolved particle number and black carbon concentrations in urban areas near Schiphol airport (the
777 Netherlands), Atmos. Environ., 104, 132-142, <http://dx.doi.org/10.1016/j.atmosenv.2015.01.015>
778
779 Lobo, P., Hagen, D.E., Whitefield, P.D. and Raper, D., 2015. PM emissions measurements of in-
780 service commercial aircraft engines during the Delta-Atlanta Hartsfield Study, Atmos. Environ.,
781 104, 237-245, <http://dx.doi.org/10.1016/j.atmosenv.2015.01.020>
782
783 Masiol, M., Harrison, R.M., Vu, T.V. and Beddows, D.C.S., 2017. Sources of sub-micrometre
784 particles near a major international airport, Atmos. Chem. Phys., 17, 12379-12403,
785 <https://doi.org/10.5194/acp-17-12379-2017>
786
787 Peters, J., Berghmans, P., Van Laer, J. and Frijns, E., 2016. UFP- en BC-metingen rondom de
788 luchthaven van Zaventem. 2016/MRG/R/0493, [https://www.vmm.be/publicaties/ufp-en-bc-](https://www.vmm.be/publicaties/ufp-en-bc-metingen-rondom-de-luchthaven-van-zaventem)
789 [metingen-rondom-de-luchthaven-van-zaventem](https://www.vmm.be/publicaties/ufp-en-bc-metingen-rondom-de-luchthaven-van-zaventem)
790
791 Riley, E.A., Gould, T., Hartin, K., Fruin, S.A., Simpson, C.D., Yost, M.G. and Larson, T., 2016.
792 Ultrafine particle size as a tracer for aircraft turbine emissions, Atmos. Environ., 139, 20-29,
793 <http://dx.doi.org/10.1016/j.atmosenv.2016.05.016>
794
795 Rizzo, M.J. and Scheff, P.A., 2007. Utilizing the chemical mass balance and positive matrix
796 factorization models to determine influential species and examine possible rotations in receptor
797 modelling results, Atmos. Environ., 41, 6986-6998,
798 <https://dx.doi.org/10.1016/j.atmosenv.2007.05.008>
799
800 Shirmohammadi, F., Sowlat, M.H., Hasheminassab, S., Saffari, A., Ban-Weiss, G. and Sioutas, C.,
801 2017. Emission rates of particle number, mass and black carbon by the Los Angeles International
802 Airport (LAX) and its impact on air quality in Los Angeles, Atmos. Environ., 151, 82-93,
803 <https://dx.doi.org/10.1016/j.atmosenv.2016.12.005>
804
805 Stacey, B., 2019. Measurement of ultrafine particles at airports: A review, Atmos. Environ., 198,
806 463-477, <https://dx.doi.org/10.1016/j.atmosenv.2018.10.041>
807
808 Stanier, C.O., Khlystov, A.Y., Chan, W.R., Mandiro, M. and Pandis, S.N., 2004. A Method for the
809 In Situ Measurement of Fine Aerosol Water Content of Ambient Aerosols: The Dry-Ambient
810 Aerosol Size Spectrometer (DAASS), Special Issue of Aerosol Science and Technology on
811 Findings from the Fine Particulate Matter Supersites Program, Aerosol Sci. Technol., 38:S1, 215-
812 228, <https://dx.doi.org/10.1080/02786820390229525>
813

814 Turgut, E.T., Cavcar, M., Yay, O.D., Ucarsu, M., Yilmaz, E., Usanmaz, O., Armutlu, K. and
815 Dogeroglu, T., 2015. A gaseous emissions analysis of commercial aircraft engines during test-cell
816 run, *Atmos. Environ.*, 116, 102-111, <http://dx.doi.org/10.1016/j.atmosenv.2015.06.031>
817

818 Vander Wal, R.L., Bryg, V.M. and Huang, C.-H., 2016. Chemistry characterization of jet aircraft
819 engine particulate matter by XPS: Results from APEX III, *Atmos. Environ.*, 140, 623-629,
820 <http://dx.doi.org/10.1016/j.atmosenv.2016.05.039>
821

822 Virkkula, A., Mäkelä, T., Hillamo, R., Yli-Tuomi, T., Hirsikko, A., Hämeri, K. Koponen, I.K.,
823 2007. A Simple Procedure for Correcting Loading Effects of Aethalometer Data, *Journal of the Air*
824 *& Waste Management Association*, 57:10, 1214-1222, [https://doi.org/10.3155/1047-](https://doi.org/10.3155/1047-3289.57.10.1214)
825 [3289.57.10.1214](https://doi.org/10.3155/1047-3289.57.10.1214)
826

827 Wang, Y., Hopke, P.K., Rattigan, O.V., Xia, X., Chalupa, D.C. and Utell, M.J. 2011.
828 Characterization of residential wood combustion particles using the two-wavelength aethalometer,
829 *Environ. Sci. Technol.*, 45, 7387-7393, <https://dx.doi.org/10.1021/es2013984>
830

831 Westerdahl, D., Fruin, S.A., Fine, P.L. and Sioutas, C., 2008. The Los Angeles International
832 Airport as a source of ultrafine particles and other pollutants to nearby communities. *Atmos.*
833 *Environ.*, 42, 3143–3155, <https://dx.doi.org/10.1016/j.atmosenv.2007.09.006>
834

835 Wiedensohler, A., Wiesner, A., Weinhold, K., Birmili, W., Hermann, M., Merkel, M., Müller, T.,
836 Pfeifer, S., Schmidt, A., Tuch, T., Velarde, F., Quincey, P., Seeger, S. and Nowak, A., 2018.
837 Mobility particle size spectrometers: Calibration procedures and measurement uncertainties,
838 *Aerosol Sci. Technol.*, 52, 146-164, <https://dx.doi.org/10.1080/02786826.2017.1387229>
839

840 Wiedensohler, A., Birmili, W., Nowak, A., Sonntag, A., Weinhold, K., Merkel, M., Wehner, B.,
841 Tuch, T., Pfeifer, S., Fiebig, M., Fjåraa, A.M., Asmi, E., Sellegri, K., Depuy, R., Venzac, H.,
842 Villani, P., Laj, P., Aalto, P., Ogren, J.A., Swietlicki, E., Williams, P., Roldin, P., Quincey, P.,
843 Hüglin, C., Fierz-Schmidhauser, R., Gysel, M., Weingartner, E., Riccobono, F., Santos, S.,
844 Gruning, C., Faloon, K., Beddows, D., Harrison, R., Monahan, C., Jennings, S.G., O'Dowd, C.D.,
845 Marinoni, A., Horn, H.-G., Keck, L., Jiang, J., Scheckman, J., McMurry, P.H., Deng, Z., Zhao,
846 C.S., Moerman, M., Henzing, B., de Leeuw, G., Lösschau, G. and Bastian, S., 2012. Mobility
847 particle size spectrometers: harmonization of technical standards and data structure to facilitate high
848 quality long-term observations of atmospheric particle number size distributions, *Atmos. Meas.*
849 *Tech.*, 5, 657-685, www.atmos-meas-tech.net/5/657/2012/ [https://dx.doi.org/10.5194/amt-5-657-](https://dx.doi.org/10.5194/amt-5-657-2012)
850 [2012](https://dx.doi.org/10.5194/amt-5-657-2012)
851
852

853 **SUPPLEMENTARY INFORMATION:**

854

855 Evaluation of Ultrafine Particle Concentrations and Size Distributions at London Heathrow Airport.

856 Supplemental information.

857

Station	Equipment installed
LHR2	API T200 NOx analyser FIDAS 200 PM analyser Magee AE33-7 Black Carbon analyser Lufft WS-600 weather station (WS/WD/T/P/RH/Precipitation)
Oaks Road	API T200 NOx analyser FIDAS 200 PM analyser Magee AE33 Black Carbon analyser

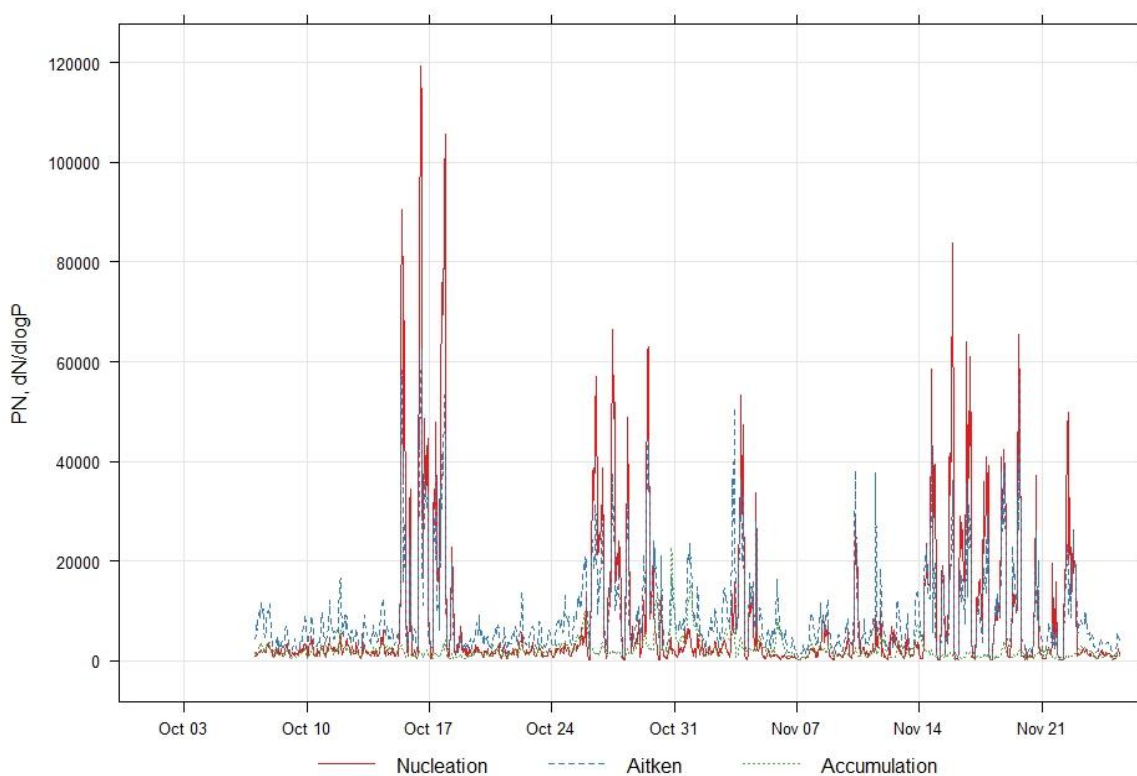
858 Table S1 – Conventional instrumentation at LHR2 and Oaks Road

859

Pollutant	Accuracy	Limit of detection
NO	±14.0%	±2ppb
NO ₂	±14.0%	±2ppb
PM ₁₀	±7.5%	±3µg/m ³
PM _{2.5}	±9.3%	±3µg/m ³
BC	±15.4%	±0.1µg/m ³
Particle Number	20%	20 particles /cm ³

860 Table S2 – Accuracy and detection limits for instruments used for the survey.

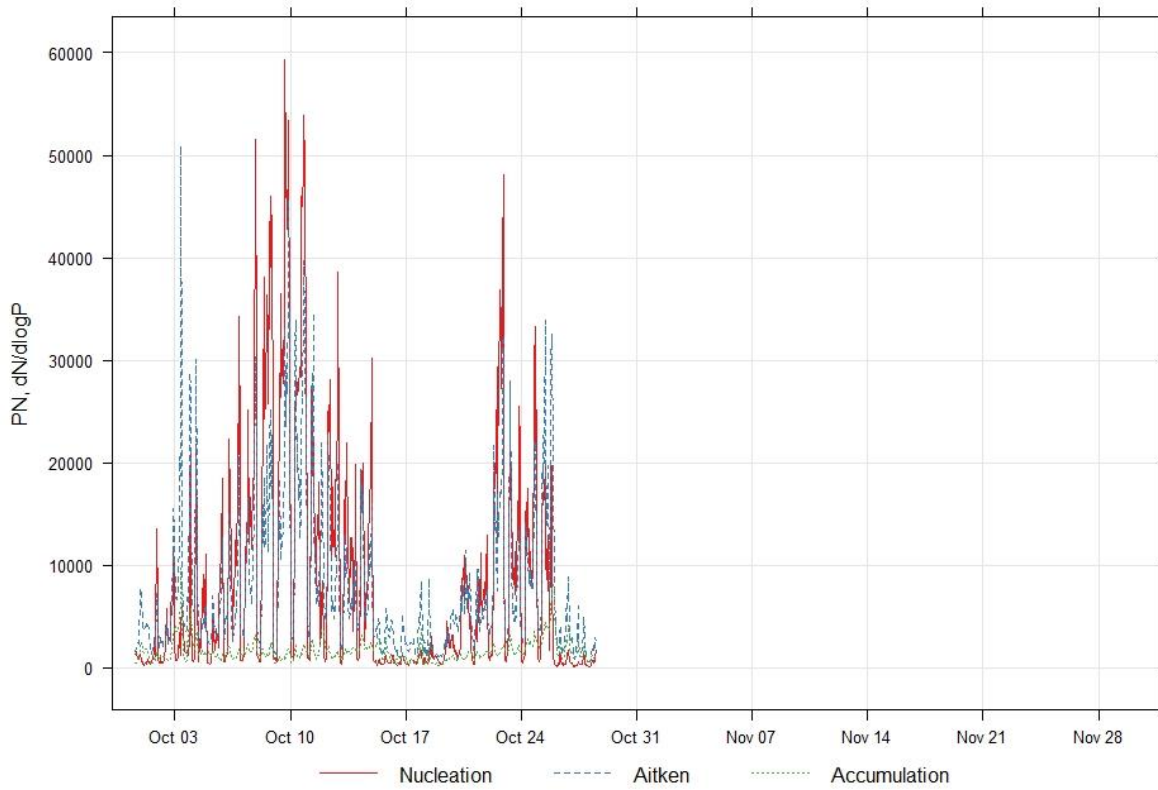
LHR 2 Timeseries Plot



861

862 Figure S1 – LHR2 PN timeseries plot

Oaks Road Timeseries Plot

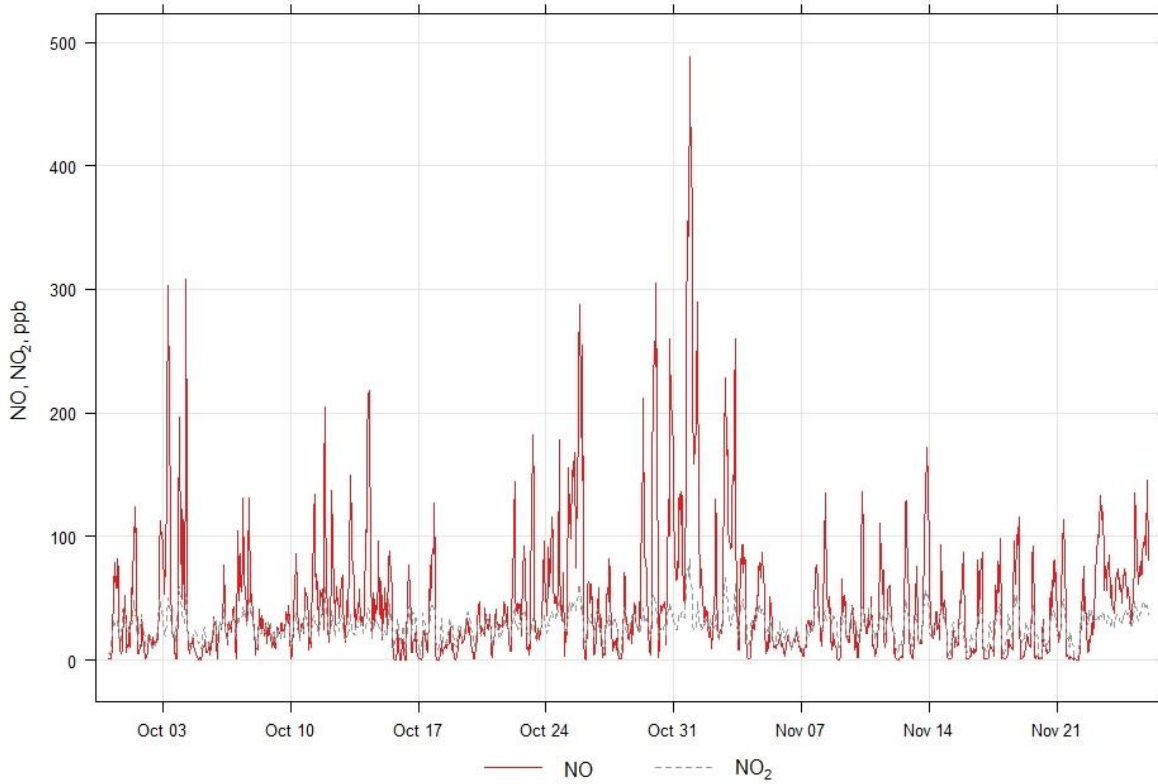


863

864 S2 – Oaks Road PN timeseries plot

Figure

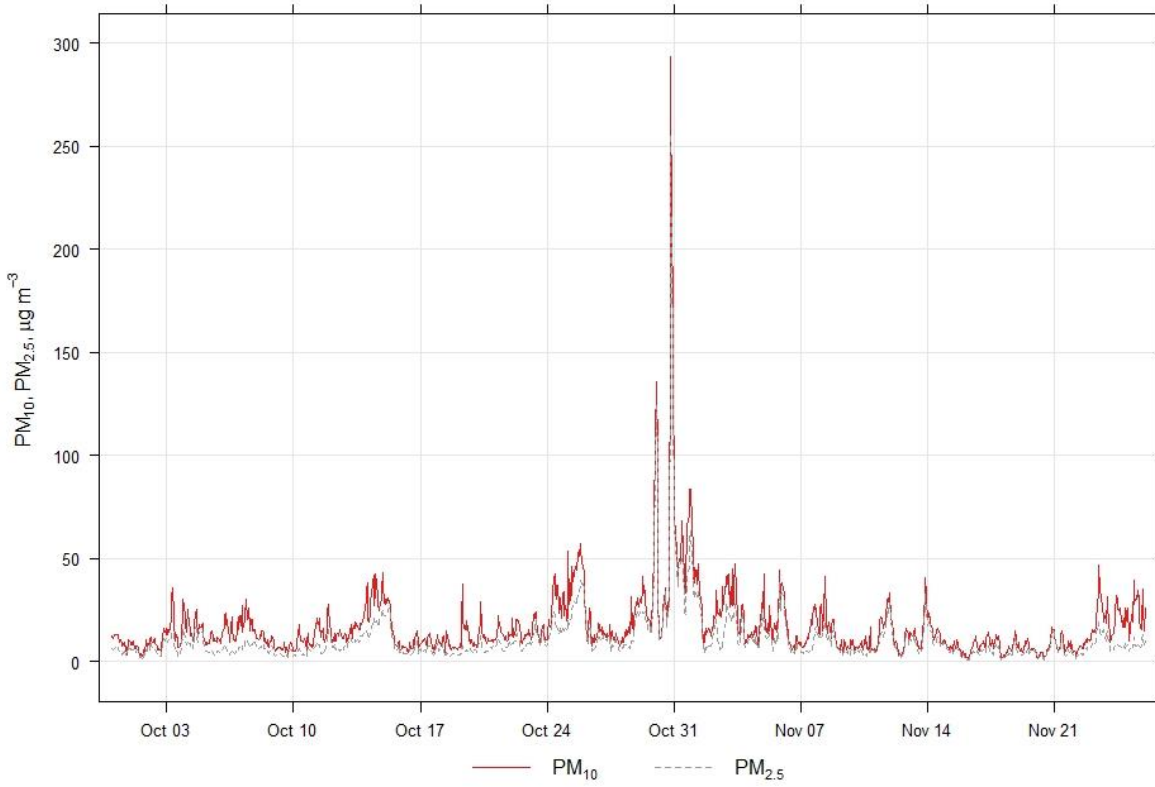
LHR 2 Timeseries Plot



865

866 Figure S3 – LHR2 NOx timeseries plot

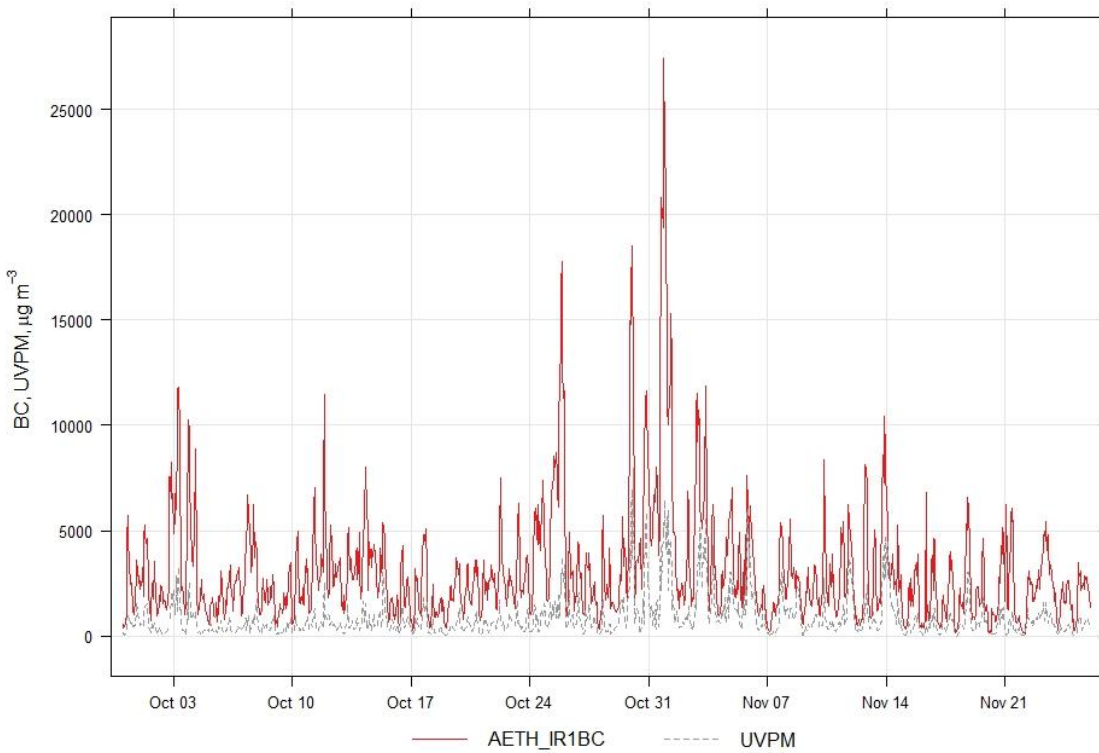
LHR 2 Timeseries Plot



867
868

Figure S4 – LHR2 PM timeseries plot

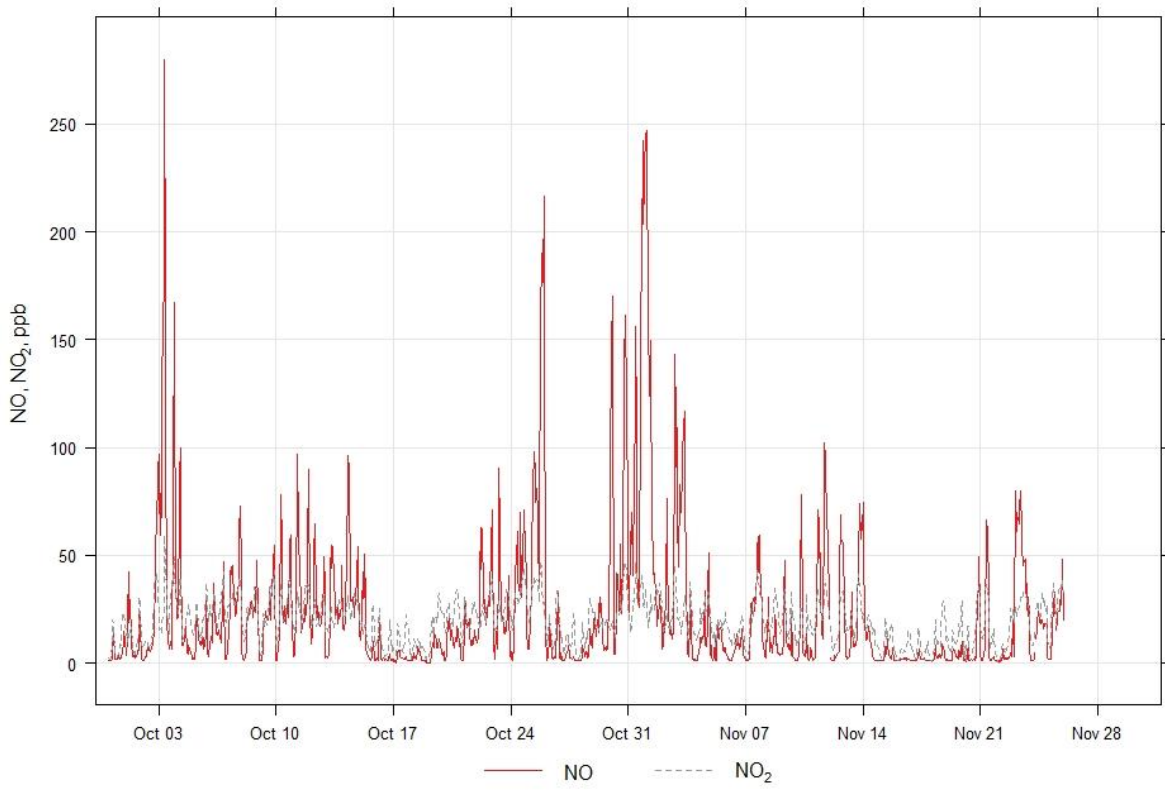
LHR 2 Timeseries Plot



869
870

Figure S5 – LHR2 BC timeseries plot

Oaks Road Timeseries Plot

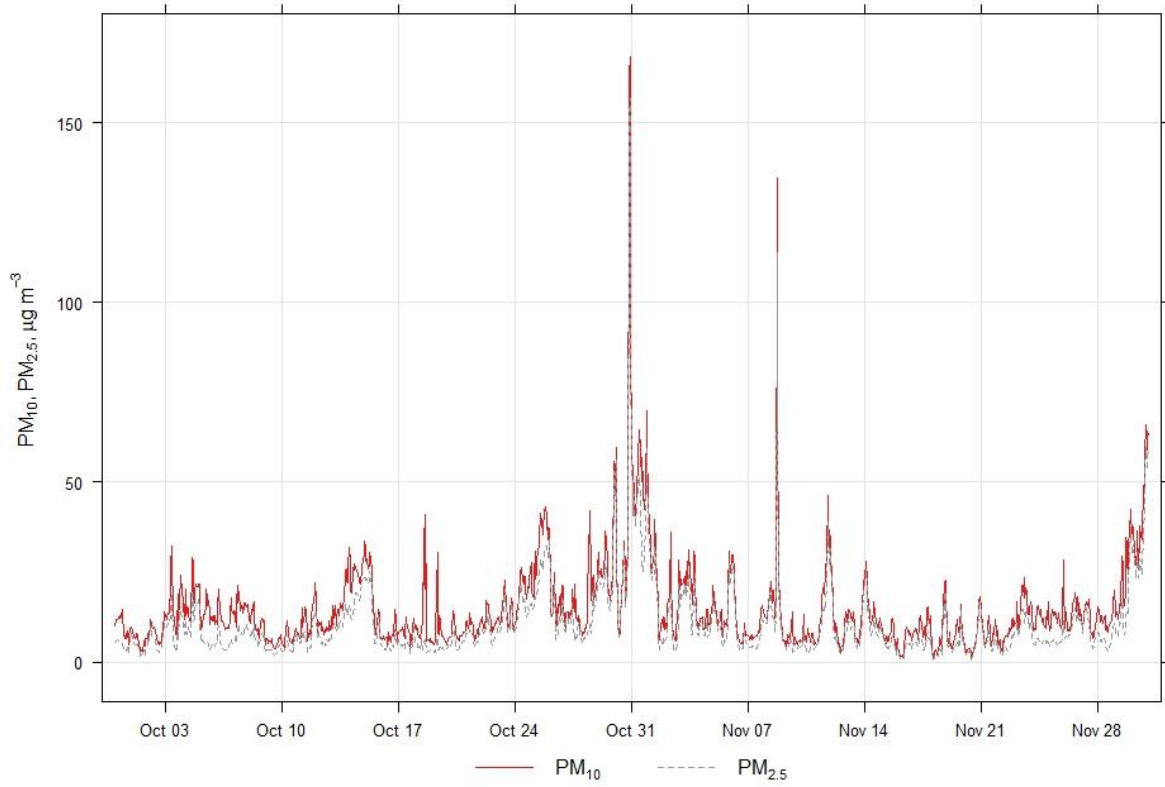


871

872 S6 – Oaks Road NOx timeseries plot

Figure

Oaks Road Timeseries Plot

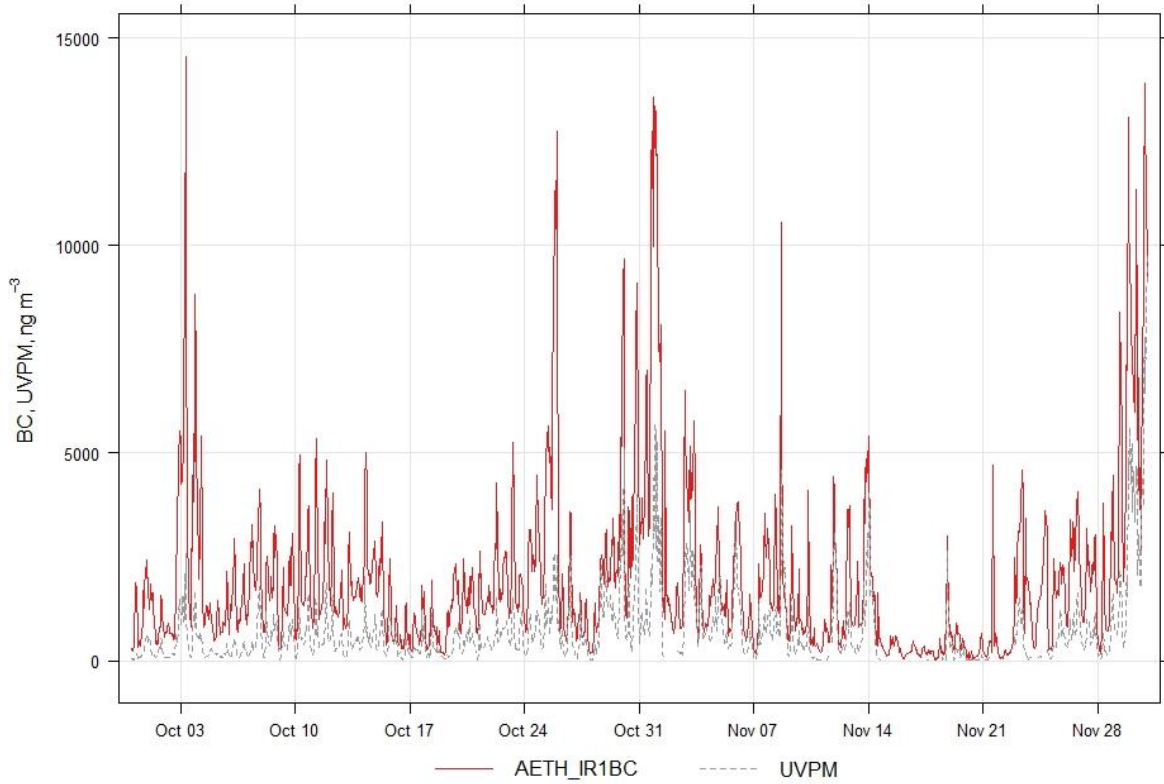


873

874 Figure S7 – Oaks Road PM timeseries plot

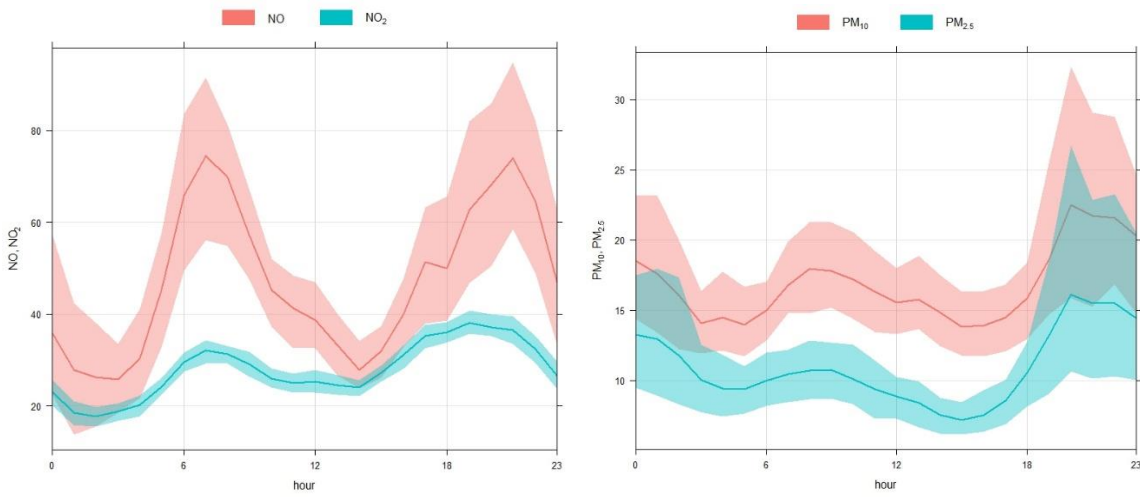
875

Oaks Road Timeseries Plot

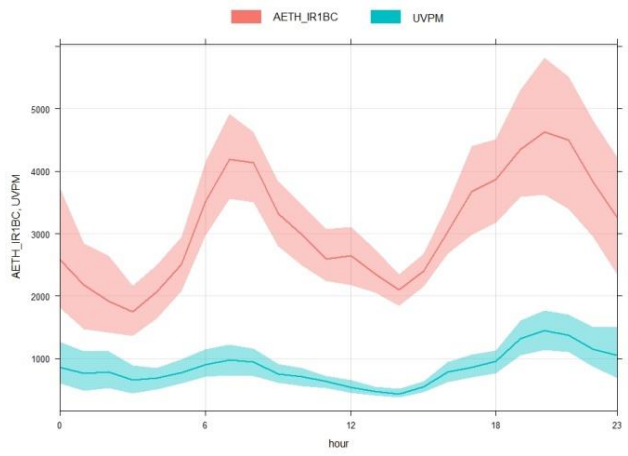
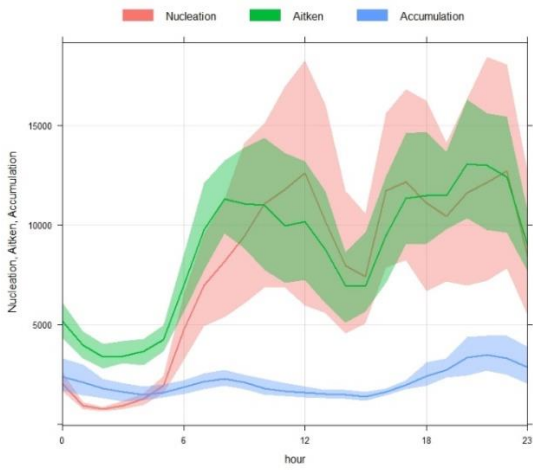


876
877
878
879

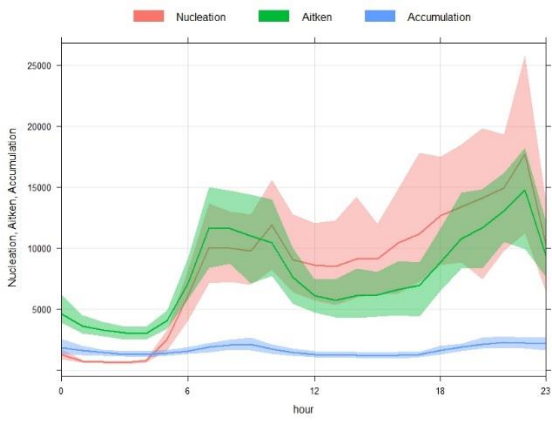
Figure S8 – Oaks Road BC timeseries plot



880

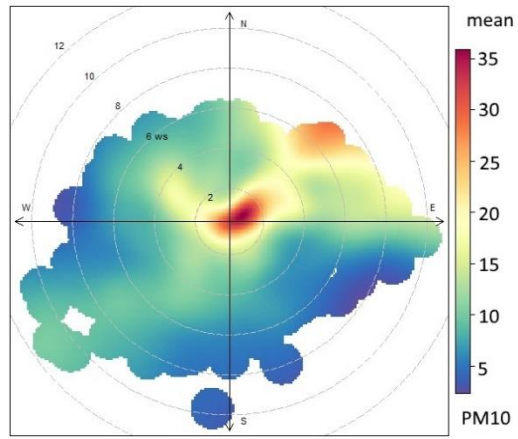
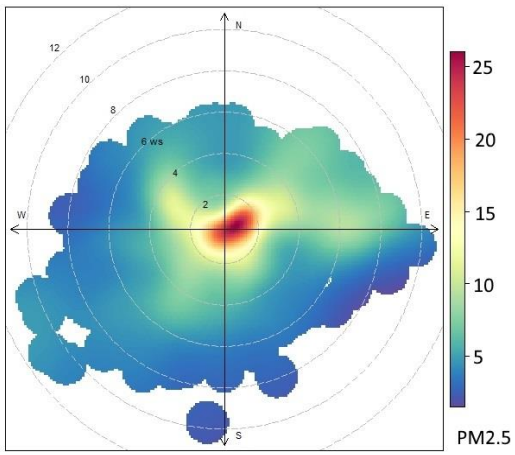


881
882 Figure S9 – Diurnal plots for measurements at LHR2
883

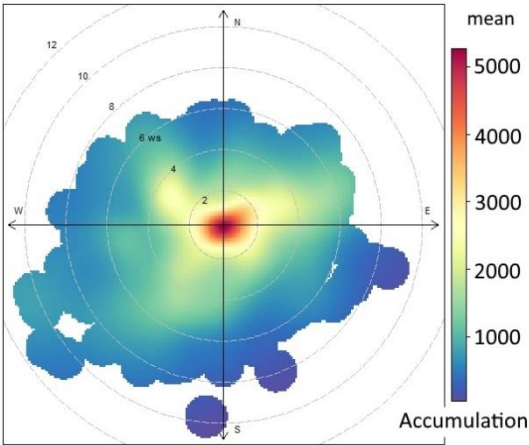
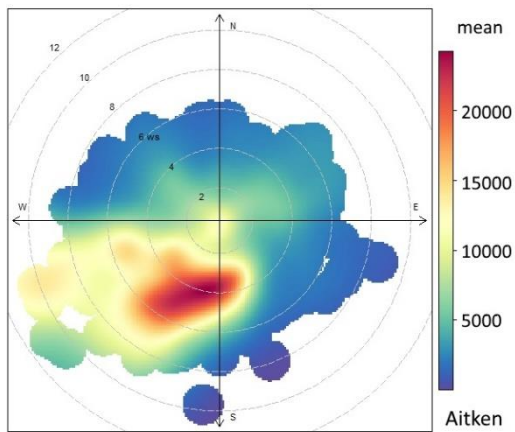


884
885 Figure S10 – Diurnal plots of Particle Number concentrations at Oaks Road
886

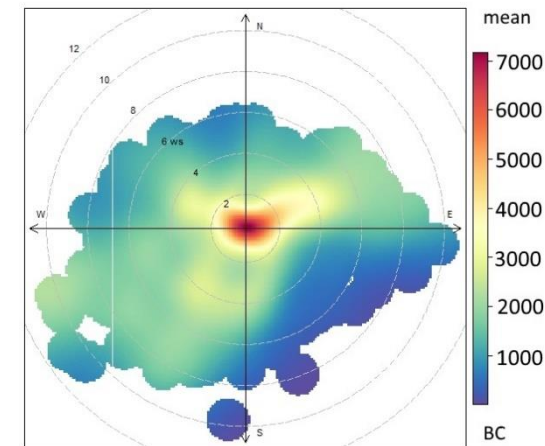
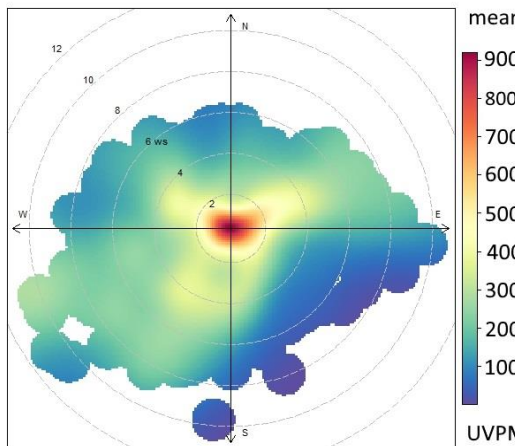
887



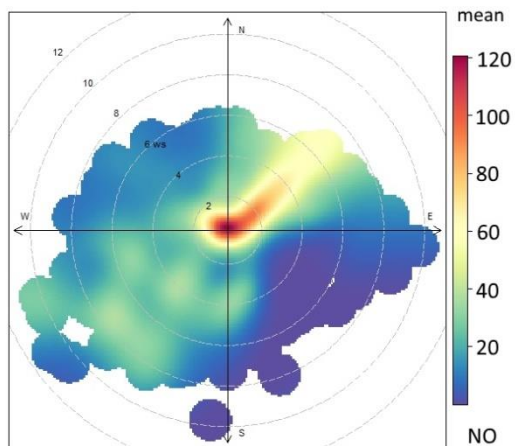
888



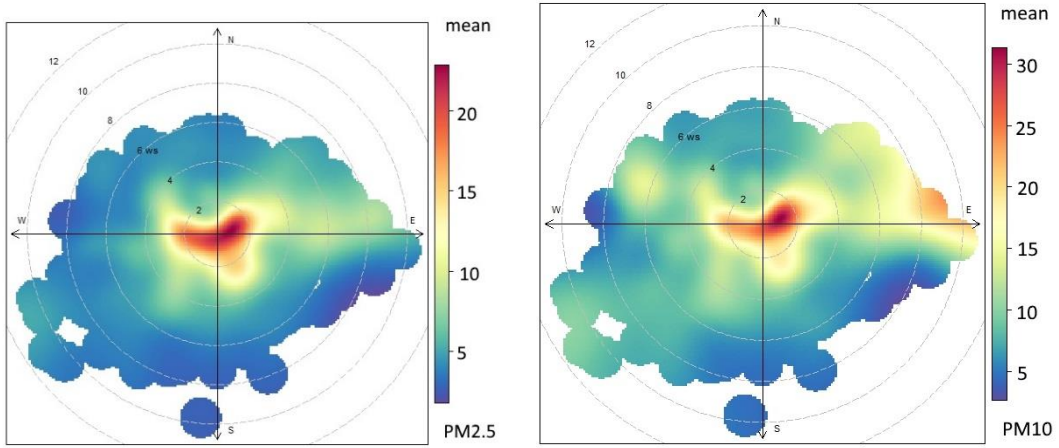
889



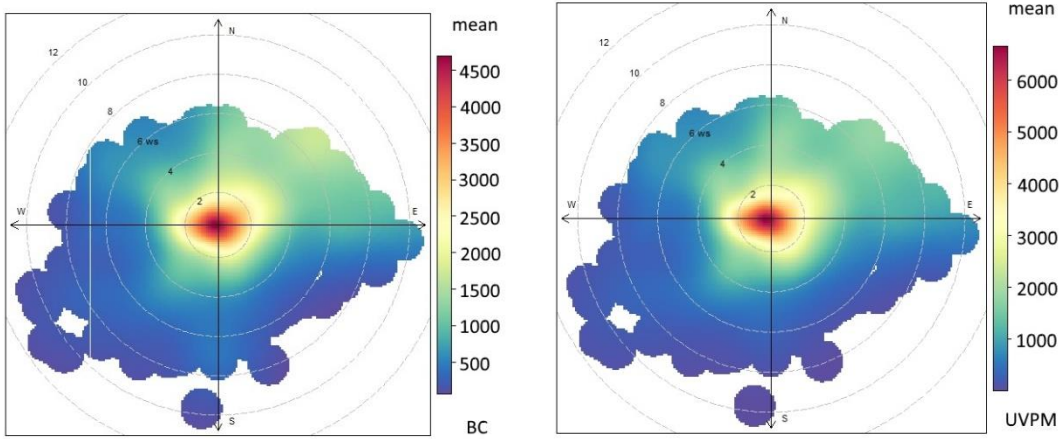
890



891 Figure S11 – Polar plots for LHR2 measurements

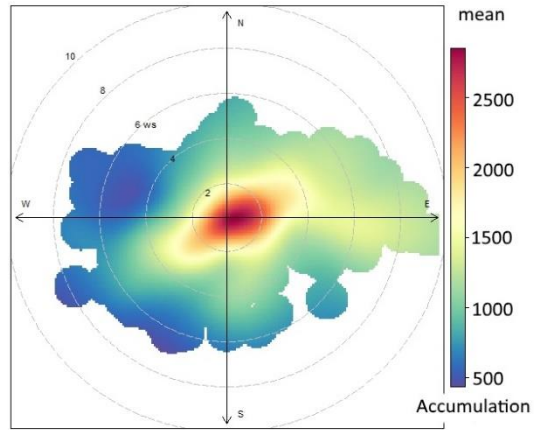
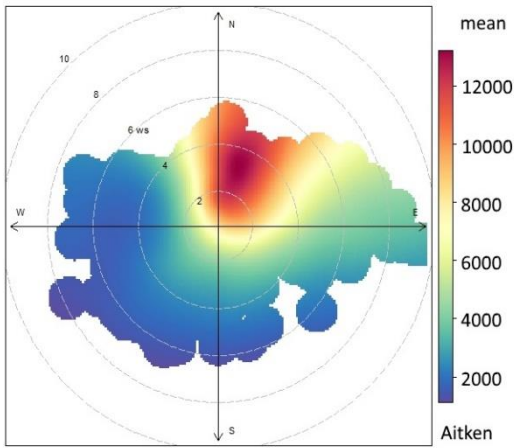


892



893

894



895
896
897

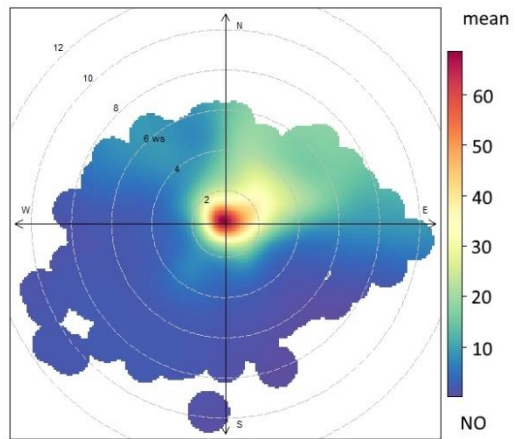
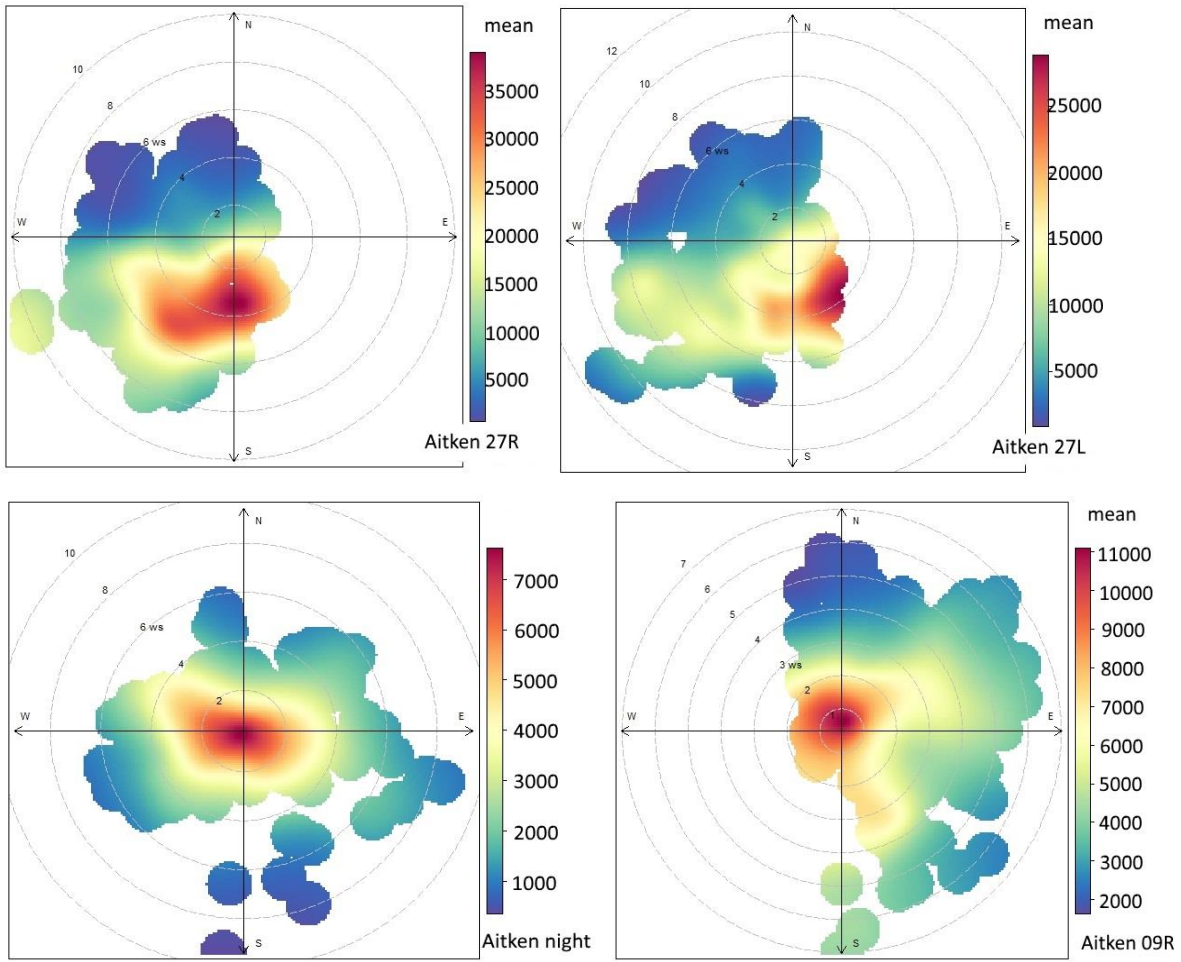


Figure S12 – Polar plots for Oaks Road measurements

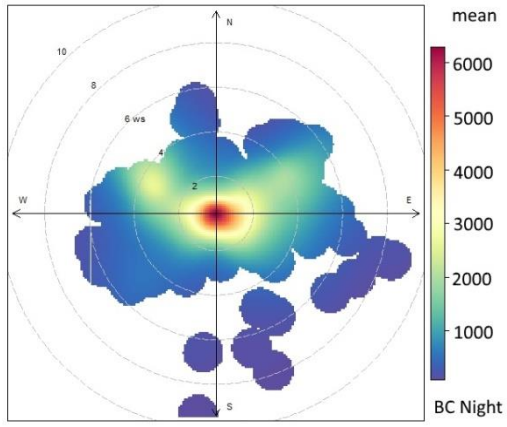
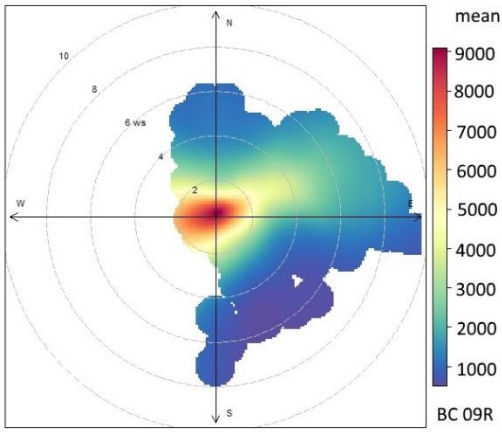
898



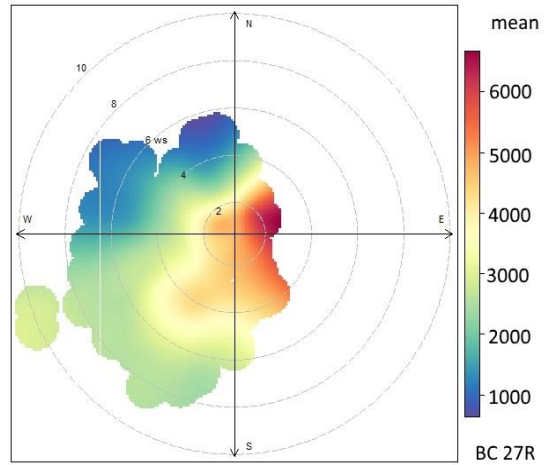
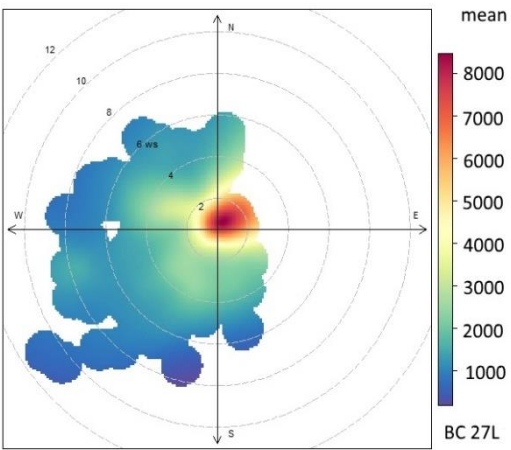
899
900
901

Figure SI13 – Aitken particle mode for LHR2, 27L, 27R, 09R and overnight modes

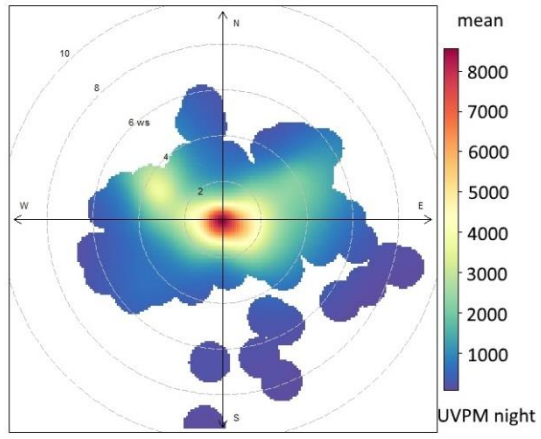
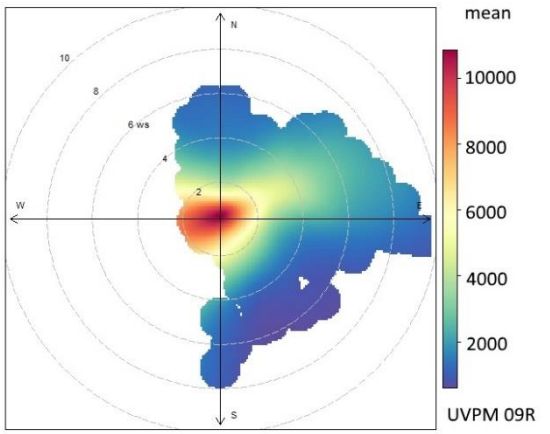
902



903

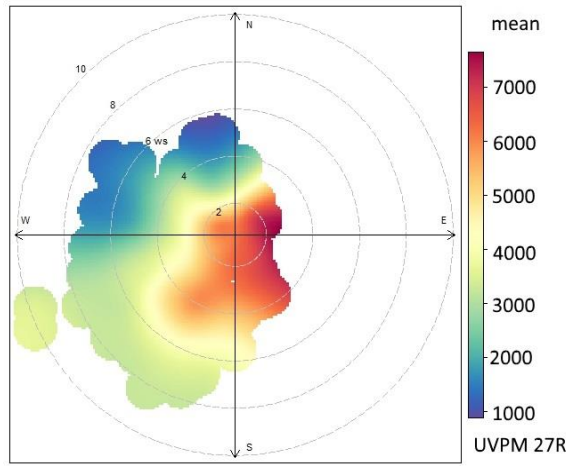
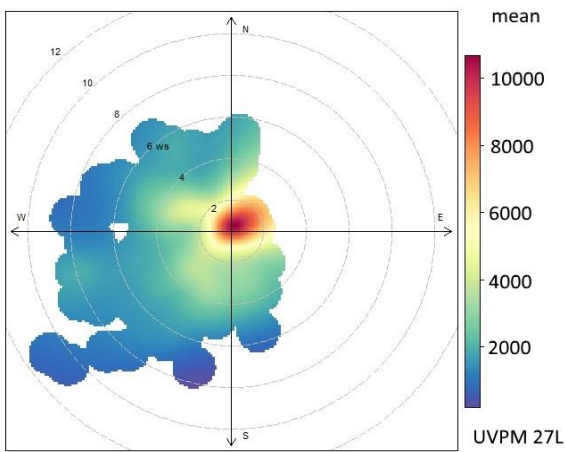


904

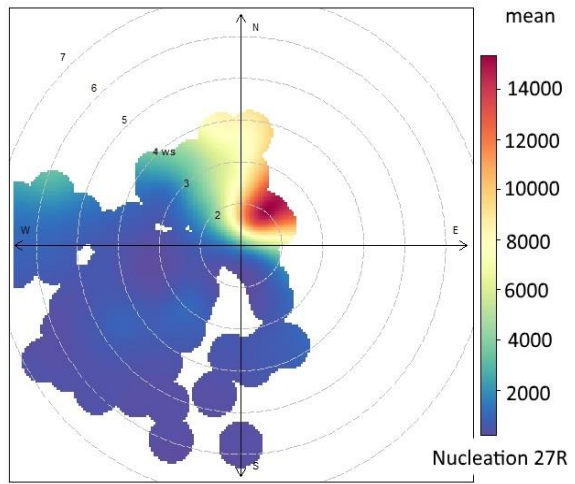
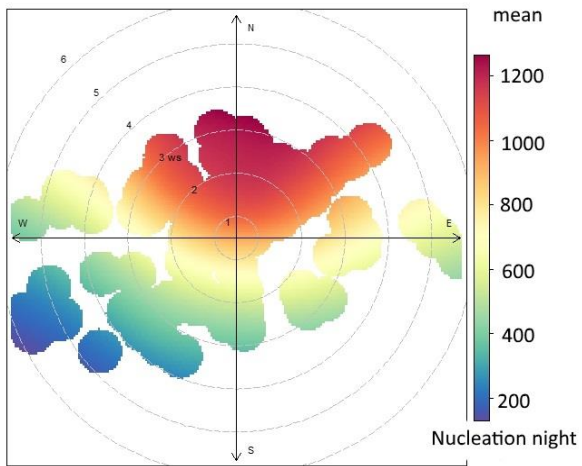


905
906
907

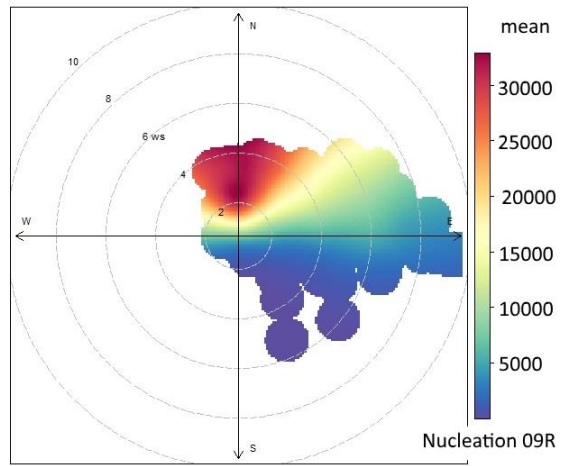
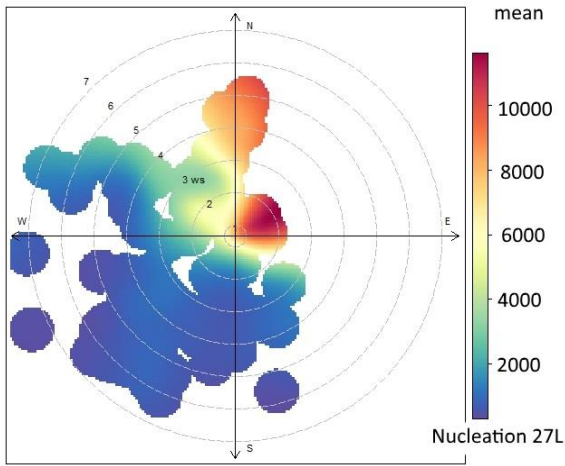
Figure S14 – Black Carbon and UVPM at LHR2 split by runway mode



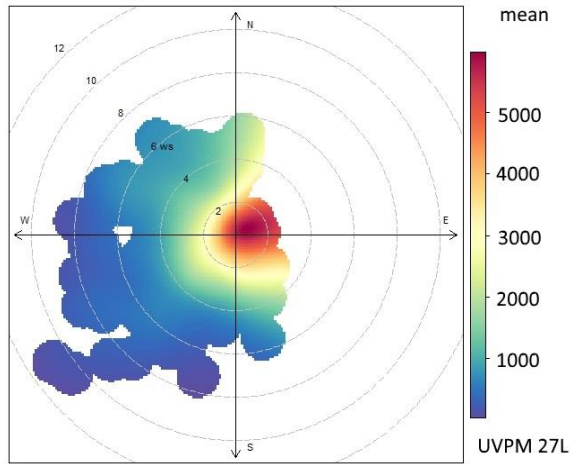
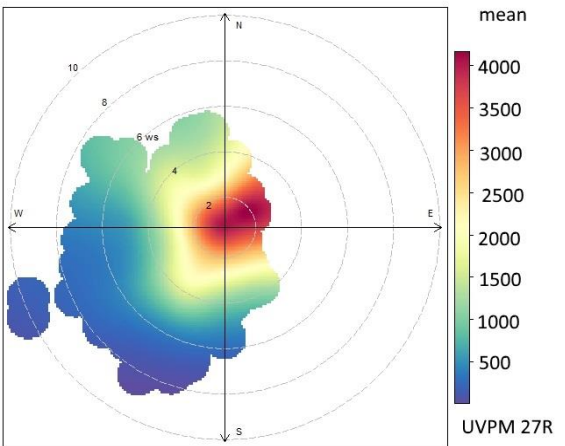
908



909



910



911
912
913
914

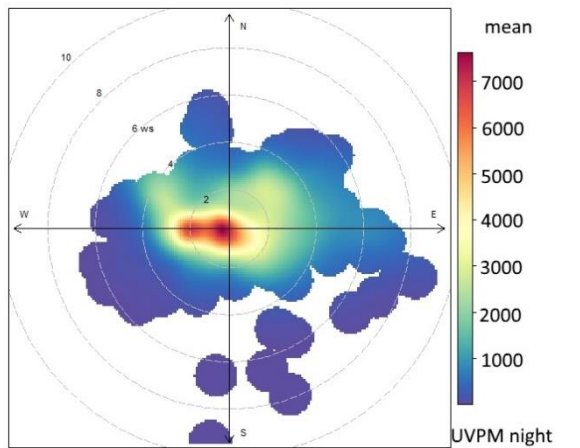
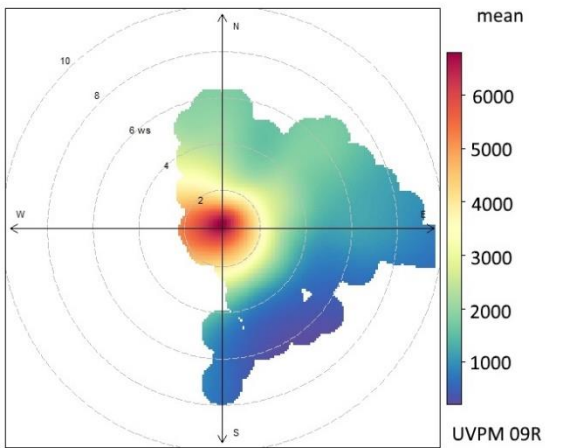
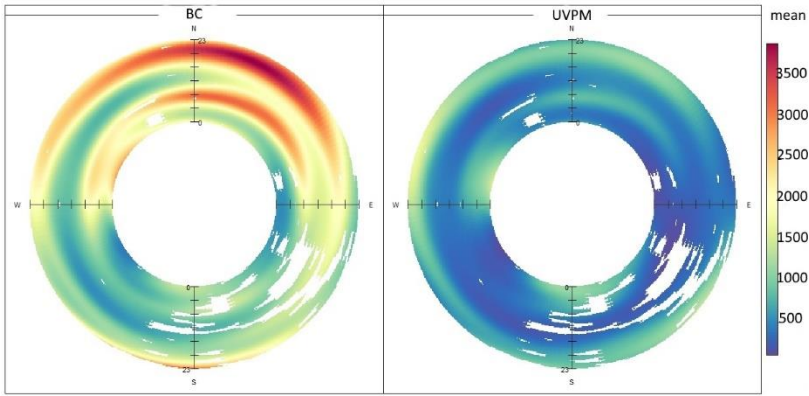
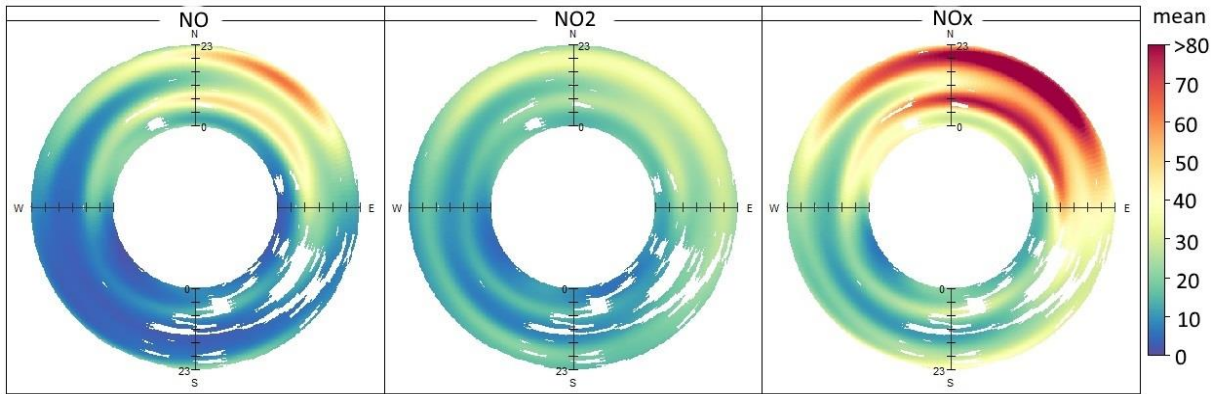


Figure S15 - Nucleation mode particles and UVPM at Oaks Road split by runway mode

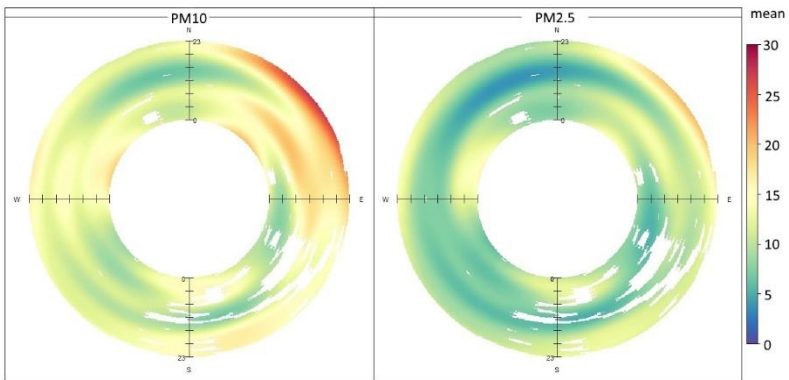
915



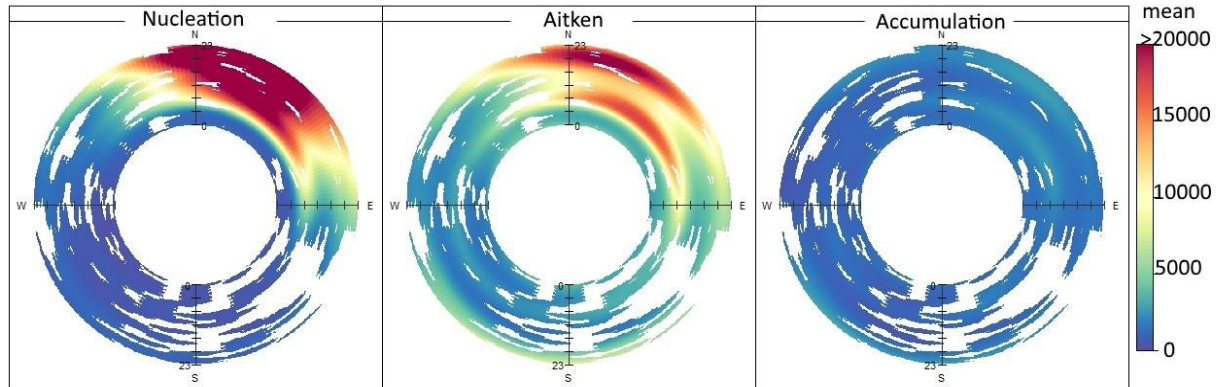
916



917

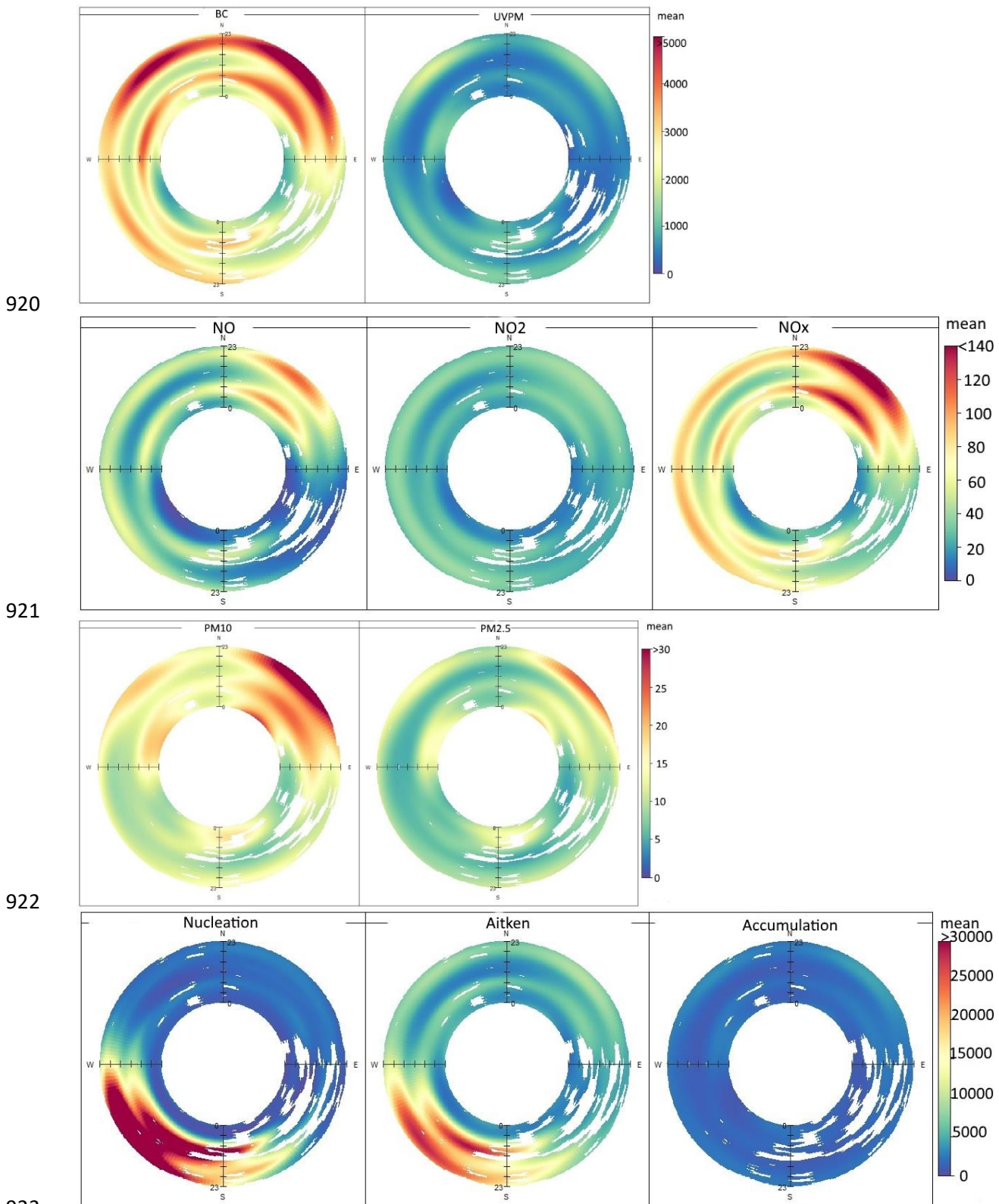


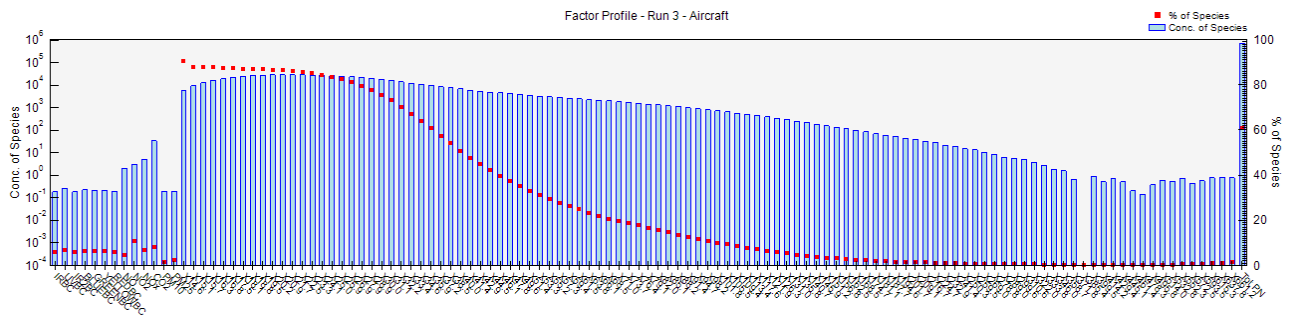
918



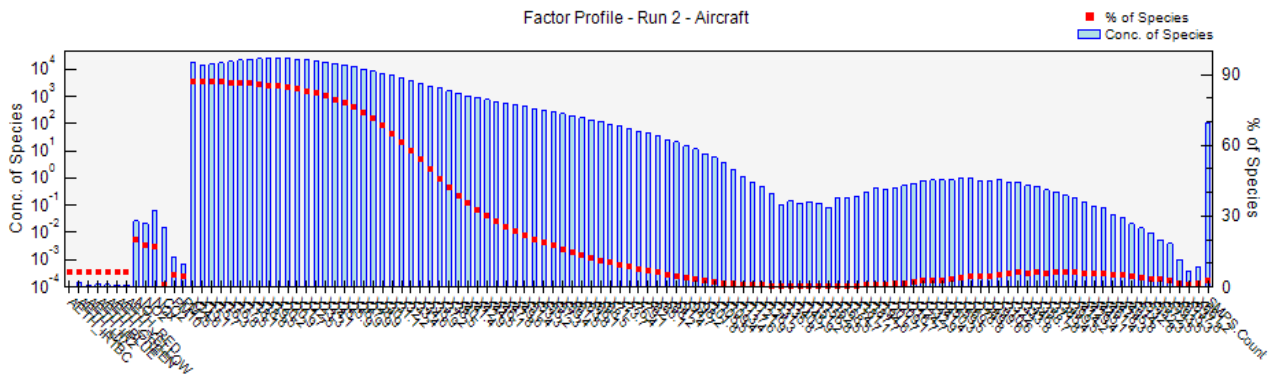
919

Figure S16 – Oaks Road Polar Annuli



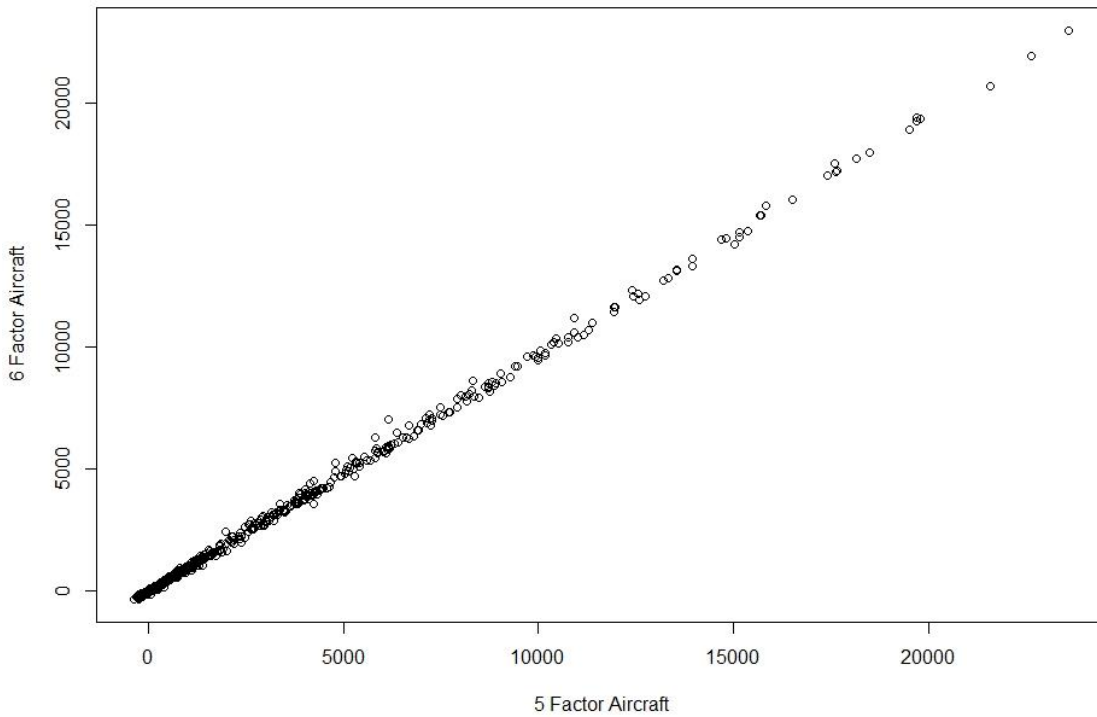


925
926 Figure S18 – PMF aircraft factor for LHR2 using all SMPS channels



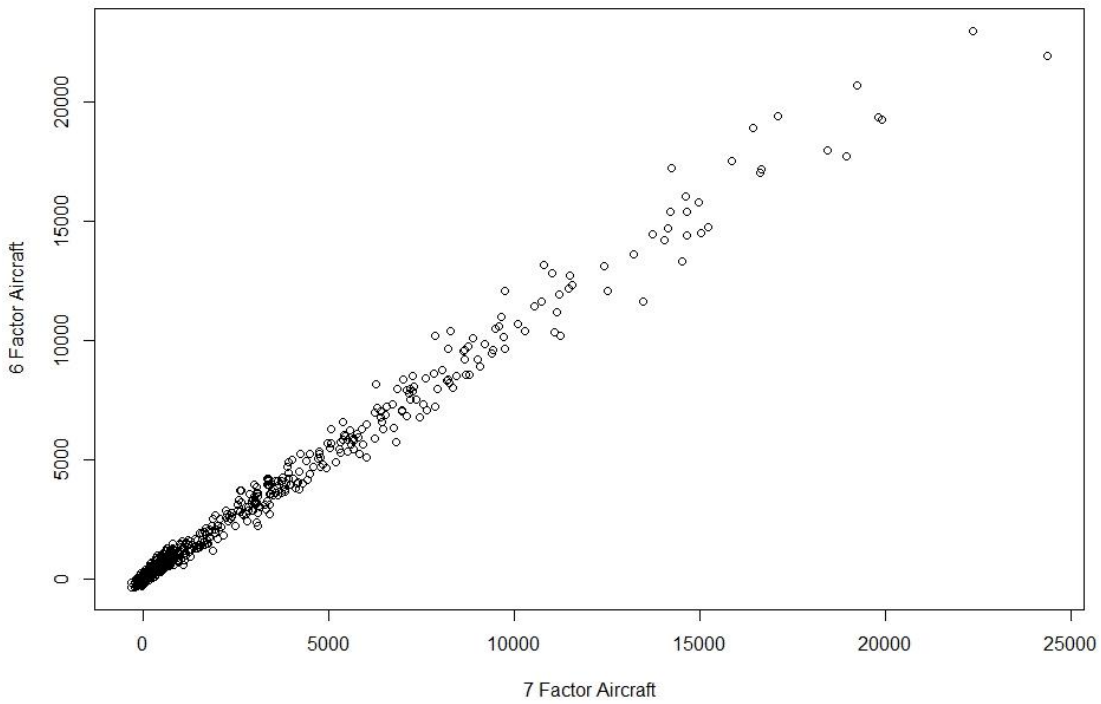
927
928 Figure S19 – PMF aircraft factor for Oaks Road using all SMPS channels

LHR2 model correlation evaluation



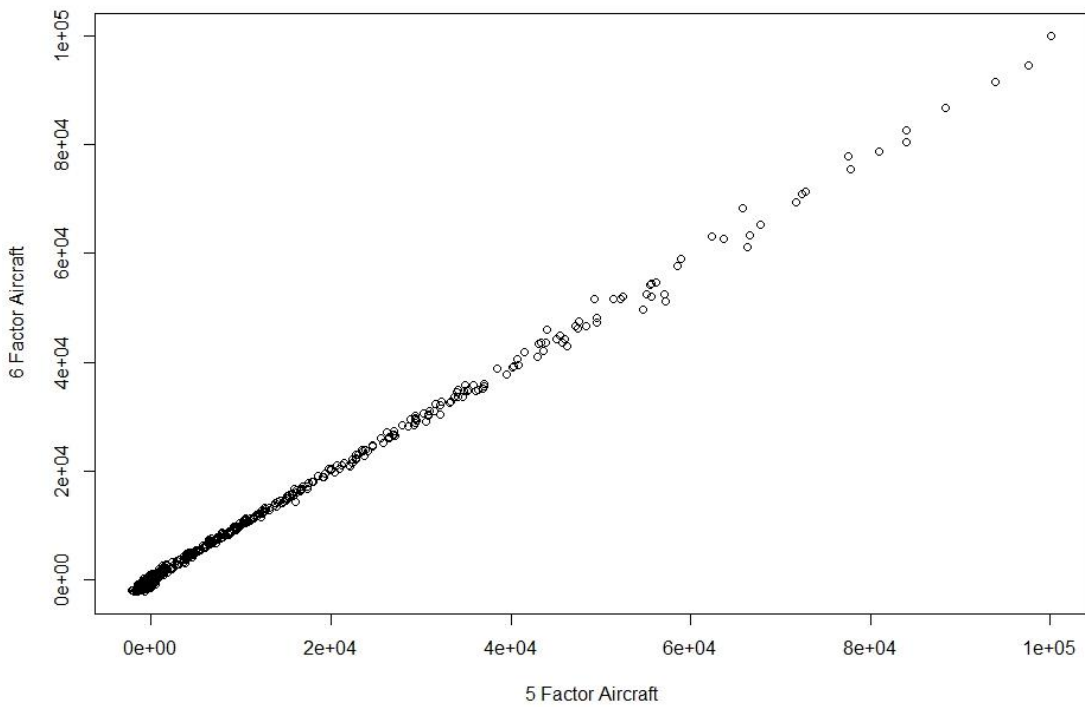
929
930 Figure S20 – Correlation between 5 and 6 factor solutions for Aircraft at LHR2

LHR2 model correlation evaluation



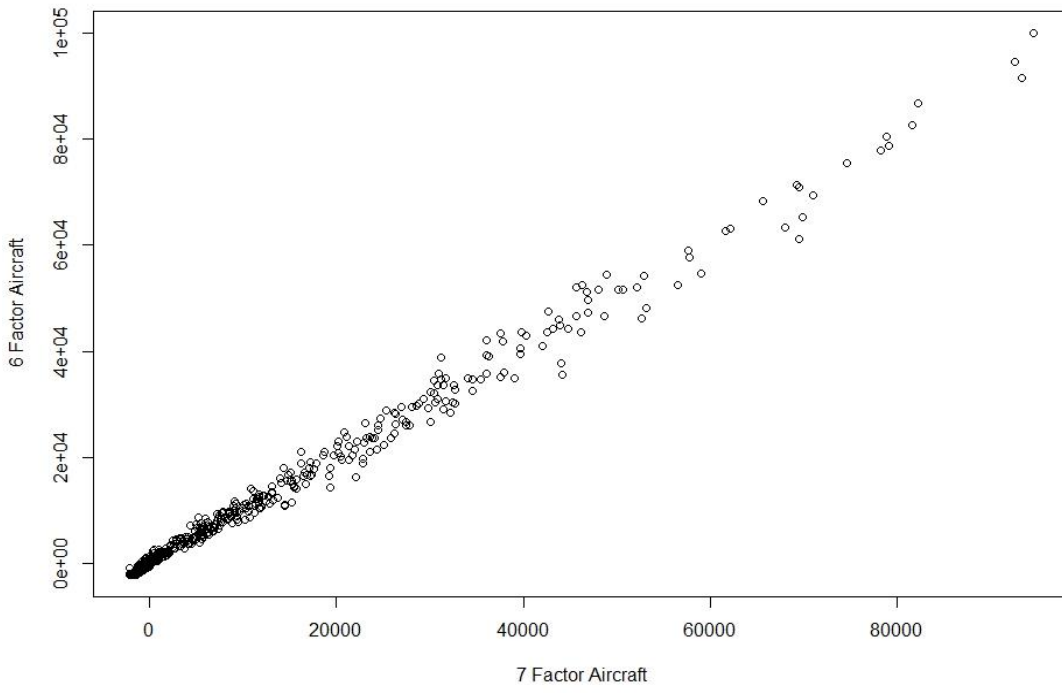
931
932 Figure S21 – Correlation between 6 and 7 factor solutions for Aircraft at LHR2

Oaks Road model correlation evaluation



933
934 Figure S22 – Correlation between 5 and 6 factor solutions for Aircraft at Oaks Road

Oaks Road model correlation evaluation



935
936 Figure S23 – Correlation between 6 and 7 factor solutions for Aircraft at Oaks Road
937
938